Favipiravir Pharmacokinetics in Nonhuman Primates and Insights for Future Efficacy Studies of Hemorrhagic Fever Viruses.

Vincent Madelain, Jérémie Guedj, France Mentré, Thi Huyen Tram Nguyen, Frédéric Jacquot, Lisa Oestereich, Takumi Kadota, Koichi Yamada, Anne-Marie Taburet, Xavier de Lamballerie, et al.

Favipiravir pharmacokinetics in non-human primates: insights for future efficacy studies of haemorrhagic fever viruses

Vincent Madelain,[a]# Jérémie Guedj,[a] France Mentré,[a] Thi Huyen Tram Nguyen,[a] Frédéric Jacquot,[b] Lisa Oestereich,[c,d] Takumi Kadota,[e] Koichi Yamada,[e] Anne-Marie Taburet,[f] Xavier de Lamballerie,[g,h] Hervé Raoul,[b]

Affiliations:

IAME, UMR 1137, INSERM, Université Paris Diderot, Sorbonne Paris Cité Paris, France [a] ; Laboratoire P4 Inserm-Jean Mérieux, US003 Inserm, 69365 Lyon, France[b] ; Bernhard Nocht Institute for Tropical Medicine, 20359 Hamburg, Germany[c] ; German Center for Infection Research (DZIF), Partner Site Hamburg, Germany[d]; Dept. Research Laboratory of Toyama Chemical Co., Ltd, Japan[e]; Hopital Bicêtre, Assistance Publique-Hôpitaux de Paris ; INSERM U1184, Center for Immunology of Viral Infections and Autoimmune Diseases, CEA, Université Paris-Sud, Kremlin Bicêtre, France[f]; UMR "Emergence des Pathologies Virales" (EPV: Aix-Marseille university - IRD 190 - Inserm 1207 - EHESP), Marseille, France[g] ; Institut Hospitalo-Universitaire Méditerranée Infection, F-13385 Marseille, France[h]

Running title: Favipiravir pharmacokinetics in non-human primates

Address correspondence to vincent.madelain@inserm.fr

Abstract

Favipiravir is a RNA polymerase inhibitor that showed a strong antiviral efficacy *in vitro* and in small animal models of several viruses responsible for hemorrhagic fever (HF) including Ebola virus. The aim of this work was to characterize the complex pharmacokinetics of favipiravir in non-human primates (NHP) in order to guide future efficacy studies of favipiravir in large animal models.

Four different studies were conducted in 30 uninfected cynomolgus macaques of Chinese (n=17) or Mauritian (n=13) origin treated with intravenous favipiravir for 7 to 14 days with maintenance doses of 60 to 180 mg/kg BID. A pharmacokinetic model was developed to predict the plasma concentrations obtained with different dosing regimens and the model predictions were compared to the EC_{50} of favipiravir against several viruses.

Favipiravir pharmacokinetics was described by a model accounting for concentration dependent aldehyde oxidase inhibition. The enzyme dependent elimination rate increased over time and

was higher in NHPs from Mauritian than from Chinese origin. Maintenance dose of 100 and 120 mg/kg BID in Chinese and Mauritian NHPs, respectively, are predicted to achieve median trough plasma free concentrations above EC_{50} of Lassa and Marburg virus until day 7. For Ebola virus higher doses are required. After day 7, a 20% dose increase is needed to compensate the increase in drug clearance over time.

These results will help rationalize the choice of the dosing regimens in future studies evaluating the antiviral effect of favipiravir in NHPs and support its development against a variety of HF viruses.

INTRODUCTION

Emerging infectious diseases leading to hemorrhagic fever (HF) with severe prognosis and large ability to spread have become a major public health concern in particular in countries with limited income. Etiologic viruses are diverse and include Ebola virus (EBOV) (1), Marburg virus (MARV) (2), Dengue virus (3), Junin virus (JUNV) (4), Crimean-Congo hemorrhagic fever virus (CCHFV) (5), Rift valley fever virus (RVFV) (6), Lassa virus (LASV) (7) and Yellow fever virus (YFV) (8). For most of these viruses no curative therapeutics exists and treatment essentially relies on supportive care (9). Considering the etiologic diversity of these HF and the fact that they do not represent a major interest for the pharmaceutical companies, it is particularly relevant to identify drugs with a broad spectrum activity. Favipiravir, a pyrazine carboxamide derivative initially developed and approved against resistant influenza in Japan (10) is a relevant candidate with several studies demonstrating its effectiveness against different HF viruses *in vitro* and in rodent models (10–18). This molecule is a RNA polymerase inhibitor, metabolized intracellularly into active form favipiravir ribosyl triphosphate, which is thought to prevent viral RNA strand extension and induce lethal mutagenesis (10). The drug efficacy against EBOV was recently evaluated in a clinical trial in Guinea (JIKI trial). The conclusion of this study was that favipiravir monotherapy merits further investigation in patients with low to medium viremia, but not in those with high viremia (19).

In order to further evaluate the efficacy of this drug, non-human primates (NHPs) remain the most relevant animal model of these infections (20). However experiments are limited by the infectious hazard, the cost and the ethical issues, which restrain the possibility to conduct large dose ranging studies with detailed pharmacological assessments. In the case of favipiravir, a drug with a complex non-linear pharmacokinetics (PK) (21) and for whom the range of EC_{50}

against HF viruses is large (Table 1) an additional difficulty is to identify relevant dosing regimen.

Here we analyzed the PK of intravenous favipiravir in cynomolgus macaques after administration of repeated doses. Based on the results of four studies, we modelled the dose concentration relationship of favipiravir, using a population approach, taking into account effects of drug non-linearity, sex, anesthesia and geographic origin. Using this model we performed simulation studies to estimate the impact of various dosing regimen on favipiravir exposure and compared the results with EC_{50} of several HF viruses.

MATERIALS AND METHODS

Four studies in cynomolgus uninfected macaques were conducted to determine the PK of favipiravir (Figure 1). Studies 1A and 1B were conducted by the manufacturer Toyama Chemicals Ltd. in Japan on macaques from China. Studies 2A and 2B were conducted by the companies SILABE and Eurofin/ADME bioanalyses in France, on behalf of the academic European Reaction consortium, on macaques from Mauritius Island. The Toyama studies protocols were written in accordance with the animal welfare bylaws of Shin Nippon Biomedical Laboratories DSR and reviewed by the Institutional Animal Care and Use Committee (approval No. 2014-0662 and IACUC063-073). Reaction studies were approved by the French research ministry (approvals 02015011614462849 and 2015062511215426V1) after favorable opinion of the C2EA35-CREMEAS ethic committee.

Drug administration. In the four studies, favipiravir was dissolved in water for injection to a final concentration of 50 mg/mL, after being added with the equivalent molar mass of meglumine. Then it was diluted with physiological saline on the day or the day before dosing, to give 40, 30, and 20 mg/mL formulations, which were administered to macaques by short intravenous infusion. In order to mimic infection studies, animals in study 1B, 2A, and 2B were anesthetized within 30 minutes before each drug administration by intramuscular injection of Zoletil (tiletamine hydrochloride salt, 2.5 mg/kg; zolazepam hydrochloride salt, 2.5 mg/kg). Favipiravir was administered without anesthesia in study 1A. In the four studies, drug administration venous access was distinct to sampling venous access to prevent any contamination.

Studies design. Study 1A was a one-week repeated IV dose PK study including nine male non-anesthetized cynomolgus macaques from China (5-7 years old, 5.1-7.9 kg). All macaques

received the same loading dose of 300 mg/kg twice a day (BID) on D1, followed by maintenance dose of 150 (N=3), 100 (N=3) or 60 (N=3) mg/kg BID, every 12 hours by short infusion of 20 min. Drug concentrations were frequently measured at D1 and D7 (before dosing, 5 and 30 min, 1, 2, 4, 6 and 12 hr after dosing, and 24 hr after dosing at D7) and twice a day before dosing between D2 and D6.

Study 1B was a two-week repeated IV dose PK study including eight female anesthetized cynomolgus macaques from China (4-5 years old, 3.3-4.3 kg). Macaques received either a loading dose of 200 mg/kg BID on D1, followed by a maintenance dose of 100 mg/kg BID (N=4) or a loading dose of 250 mg/kg BID on D1, followed by a maintenance dose of 150 mg/kg BID (N=4), every 12 hours by short infusion of 10 min. Drug concentrations were frequently measured on D1, D7 and D14 (before dosing, 5 and 20 min, 1, 2, 4, 8 and 12 hours after dosing, and 5 min after the second dosing at D1 and D7, 24 hr after dosing at D14) and three times a day the other days (before dosing, 5 min after dosing and before second dosing).

Study 2A was a two-week repeated IV dose PK study including five female anesthetized cynomolgus macaques from Mauritius Island (3.8-3.9 years old, 3.5-4.8 kg). All macaques received a loading dose of 200 mg/kg BID on D1, followed by a maintenance dose of 100 mg/kg BID, every 12 hours by short infusion of 10 min. Drug concentrations were frequently measured on D1 and D14 (before dosing, 5 and 20 min, 2, 4, 8 and 12 hours after dosing, 5 min after the second dosing, 24 hr after second dosing on D14) and two times a day the other days (before second dosing and 5 min after second dosing).

Study 2B was a one-week repeated IV dose PK study including eight female anesthetized cynomolgus macaques from Mauritius Island (3.4-4.7 years old, 3.6-4.8 kg). Macaques received either a loading dose of 250 mg/kg BID on D1 followed by a maintenance dose of 150 mg/kg BID (N=4) or a loading dose of 250 mg/kg BID on D1 followed by a maintenance dose of 180 mg/kg BID (N=4), every 12 hours by short infusion of 10 min. Drug concentrations were frequently measured on D7 (before dosing, 5 min, 2, 4, 8 and 12 hours after dosing), four times a day on D1 and D2 (before and 5 min after first and second dosing) and three times a day the other days (before and 5 min after first dosing, before second dosing).

Safety. Clinical signs, body weight and food consumption were assessed daily. Hematology and blood chemistry parameters, including hemoglobin concentration, red cells, white cells and platelet count, reticulocyte count, serum creatine kinase, AST, ALT, bilirubin, creatinine, nitrogen urea, sodium, potassium, chlorine and calcium were assayed on pretreatment period

and at the end of the follow-up. All animals were euthanized on the last day of the study, and necropsied in studies 1B, 2A and 2B, but not in study 1A.

Analysis methods and cross validation of favipiravir concentration assay. Favipiravir plasma concentrations were assayed separately in studies 1 and 2, using respectively high performance liquid chromatography (HPLC) coupled to UV detection (Shimadzu 10A, SPD 10A) and HPLC coupled to tandem mass spectrometry detection (Kromasil C18, API4000), with limit of quantification (LOQ) of 0.1 mg/L and 5 mg/L respectively. Cross validation of the two analytical processes was blindly performed on 15 samples (see supplementary material).

Non compartmental analysis. For each animal the maximal concentrations (C_{max}), the predose concentrations (C_{trough}), the average concentrations (C_{ave}), defined as $AUC_{0\text{-}12h}$ divided by 12, and clearance (CL), defined as Dose/AUC, were obtained by non-compartmental approach, after the first administrations on day 1, day 7 and/or day 14 (see supplementary). Medians and ranges parameters in each study were reported and Wilcoxon tests were used for statistical comparisons between groups.

Modelling favipiravir pharmacokinetic in cynomolgus macaques. A PK model of favipiravir concentrations in cynomolgus macaques was developed using the strategy depicted in Figure 2.

Pharmacokinetic and residual error models were selected using data of the one-week study 1A. We started with a mono-compartmental model with linear elimination. Because a non-linearity was observed in the non-compartmental analysis (see results), we also tested a model with a Michaelis–Menten elimination, a model with both zero order and first order elimination, a model with both first order and Michaelis–Menten eliminations and a model with both first order and nonlinear eliminations depending of favipiravir plasma concentration levels (see equation 1), accounting for the aldehyde oxidase pathway. All these models were tested assuming exponential random effects on all parameters with a diagonal variance matrix for the random effects.

Next data from study 1B were added; as it was a two-week study, time effect was tested on elimination and enzyme parameters. Additions of linear, inverse tangent and exponential time function on elimination and enzyme parameters, as well as feedback effect on enzyme production, were tested. The effect of sex and anesthesia (since the design of the studies does not allow to separate them) was evaluated. Finally data from studies 2A and 2B were added and

158 the parameters were re-estimated to assess the effect of NHP origin (China and Mauritius Island
159 for studies 1 and 2, respectively) and relevant random effects were selected.

160 Model estimation was performed using nonlinear mixed effect model and the software Monolix
161 4.2.2. (http://www.lixoft.eu/) (22). Structural, covariate and residual error model selection was
162 based on the Bayesian Information Criterion (BIC) value, a fitting criterion based on the model
163 likelihood that takes into account the number of parameters in the model. Random effects with
164 a variance smaller than 0.1 or associated with a relative standard error larger than 100% were
165 deleted using a backward procedure. Correlation for random effect were added on the final
166 model on parameters presenting Pearson correlation coefficient larger than 0.6 between their
167 individual predictions. Selection of covariate effect on structural parameters was performed
168 using a forward procedure, where covariate was added sequentially on each parameter. The
169 procedure continued until no improvement in BIC was obtained. Maximum likelihood
170 estimation took into account the information brought by data under the LOQ, as described in
171 (23). Model assessment was performed throughout the model building using diagnostic plots:
172 observations *vs* population predictions, observations *vs* individual predictions, individual
173 weighted residual over time and individual predictions, normalized prediction distribution
174 errors over time and individual predictions, and visual predictive check per dose (24, 25).

175 **Simulation studies with different dosing regimens.** We used the final PK model to evaluate
176 by simulation the drug exposure that could be achieved during two weeks of favipiravir with a
177 loading dose of 200 or 250 mg/kg BID the first day followed by a maintenance dose from 60
178 to 180 mg/kg BID. In order to take into account the possible reduction in drug concentration
179 over time (see results), we also evaluated scenarios where the dosing regimen increased in the
180 second week of treatment. For each scenario 5,000 in silico PK profiles with frequent sampling
181 measurements were generated using mlxR package (http://simulx.webpopix.org/mlxr/) and
182 daily C_{ave}, C_{trough} and C_{max} were provided.

183 **Drug exposure and EC_{50} of favipiravir against hemorrhagic fevers.** The *in vitro* EC_{50} for
184 favipiravir against a variety of hemorrhagic fevers is reported in Table 1. When several EC_{50}
185 were reported in the literature, we chose to be conservative and only the highest value was
186 considered. Then we compared the median predicted drug concentrations profiles with the EC_{50}
187 of the literature. Consistent with what had been done before, we relied on free drug
188 concentrations, assuming a protein binding rate of 50% in cynomolgus macaques (Toyama in
189 house documentation) close to the value in human (54%) (26).

For MARV, given no information was available, cell culture experiments were performed purposely (see supplementary material). Favipiravir EC_{50} and EC_{90} were found equal to 6.8 and 11.4 µg/mL, respectively, in cell culture experiments (see supplementary).

RESULTS

Safety. No animals died and no toxic effect was found on the necropsy. Transient lack of faeces, vomiting, and stereotypic movement disorder (repeated backward head movements) were noted. Drop in the hemoglobin blood level, associated to increase of reticulocyte count, was observed in the four studies, with median (min-max) variation of -2.3 (-0.8;-3.2) g/dL and -1.3 (0.2; -4) g/dL from baseline to D7 in studies 1A and 2B, respectively, and -2.3 (-1.4; -2.8) g/dL and -2 (-0.9;-2.5) g/dL from baseline to D14 in studies 1B and 2A. In study 1B, in macaques receiving 150 mg/kg BID, the food consumption decreased continuously during the dosing period, leading to dosing discontinuation on day 11. However, there were no abnormalities in body weights, serum electrolyte concentrations or general status. In the study 2A macaques receiving 100 mg/kg BID, a moderate increase of creatinine concentration (+18.6 µmol/L) was observed at the end of follow-up. However, this biological abnormality was not found in groups receiving higher dosing of 150 and 180 mg/kg BID. In conclusion, no serious abnormalities were observed at the different dose regimens explored in the four studies. More details can be found in the supplementary material.

Non-compartmental analysis. The results showed a strong non-linearity of favipiravir over doses and time in Chinese cynomolgus macaques in studies 1A and 1B (Table 2). Clearance at D7 decreased with dose, from 0.13 L/h/kg to 0.04 L/h/kg for 60 mg/kg BID to 150 mg/kg BID, respectively. Data from study 1B showed in addition a non-linearity over time, with a 80% decrease of clearance between day 1 and day 7, occurring from the second administration, and then a 25% increase in clearance between days 7 and 14, for the two levels of maintenance dose.

A significantly lower exposure was found in studies 2A and 2B performed in macaques from Mauritius Island, with C_{ave} on day 14 of 47.9 mg/L compared to 102.2 mg/L for the maintenance dose of 100 mg/kg BID (p=0.040), and a C_{ave} on day 7 of 187.1 mg/L compared to 241.4 mg/L for the maintenance dose of 150 mg/kg BID (p=0.024).

PK model building. A one-compartment model with first order elimination was inadequate to describe the favipiravir PK over 7 days repeated administrations. Addition of a nonlinear Michaelis-Menten elimination term improved the fit of the data but it did not allow to describe the concentration increase from the first to the second administration. Finally, a model including enzyme mediated elimination with concentration dependent inhibition, described in Equation 1, provided the best description of the PK profiles of favipiravir and a combined residual error model was retained:

$$\frac{dA_c}{dt} = -k \times A_c - k_{enz} \times A_e \times A_c$$
$$\frac{dA_e}{dt} = R_{in} - k_{out} \times (1 + C_c \times \alpha_{deg}) \times A_e \qquad \text{Eq.1}$$
$$R_{in} = k_{out} \times A_{e0}$$
$$C_c = \frac{A_c}{V}$$

where A_c is the amount of favipiravir in central compartment, C_c the favipiravir plasma concentration, A_e the enzymatic activity level, k the first order elimination rate, k_{enz} the enzyme dependent first order elimination rate, k_{out} the enzyme elimination rate, R_{in} the zero-order enzyme synthesis rate and α_{deg} the favipiravir concentration linear effect on enzyme elimination rate. Activity level of enzyme at baseline A_{e0} was set to 1. This model makes the assumption that favipiravir increases enzyme degradation, in accordance with the irreversible inhibition mechanism proposed by the manufacturer.

Next, data of study 1B, where female cynomolgus macaques were treated and anesthetized daily for the 14 days, were included. Because the model predicts that the drug rapidly reaches steady-state it could not capture the decrease in drug concentrations between day 7 and day 14. To account for this feature a time dependent variation in enzyme kinetic on α_{deg} was added:

$$\frac{dA_e}{dt} = R_{in} - k_{out} \times (1 + C_c \times \alpha_{deg} \times e^{-\lambda \times t}) \times A_e \qquad \text{Eq.2}$$

This model has one additional parameter, λ, which is the rate at which enzyme elimination becomes less and less sensitive to favipiravir concentration. Thus, with this model, the enzyme activity increases over time and returns to its baseline value, leading to a decrease in drug concentration. Effect of the sex and/or anaesthesia was then explored using this model and selected on k_{out}.

Lastly, data from study 2A and 2B were included and the faster drug elimination in macaques from Mauritian origin was attributed to larger values of k_{enz} and α_{deg} (Table 2). Selection of the random effect led to fixing k_{out} and α_{deg} and the final model had four independent random effects. Individual fits (Figures 3 and A5) and diagnostic plots of the final model did not point any misspecification (See Figures A6, A7, A8 in the supplemental material).

Model predictions. At the first administration of favipiravir, the enzyme dependent elimination part is much larger than the independent one, with k_{enz} and k equal to 2.85 and 0.065 h^{-1}, respectively (Table 3). However the inhibition of the enzyme by favipiravir leads to a rapid decrease of the enzyme dependent pathway. The enzyme is continuously synthetized at a rate R_{in} equal to 0.024 h^{-1} and consequently it takes about 4 days after complete drug elimination to return to baseline enzyme level. Sex difference was found on parameter k_{out}, equal to 0.024 h^{-1} in female and 0.036 h^{-1} in male (Likelihood ratio test (LRT) $p = 3.10^{-6}$) In order to fit the decrease in drug concentration after repeated administration of favipiravir, we estimated λ at 0.0016 h^{-1} (Table 3). Regarding differences between the two geographic origins, cynomolgus macaques from Mauritius Island had a larger enzyme dependent elimination constant than Chinese macaques (k_{enz} equal to 2.85 h^{-1} and 1.25 h^{-1}, respectively, LRT $p = 5.10^{-5}$), and a higher favipiravir concentration linear effect on enzyme elimination rate (α_{deg} equal to 0.179 vs 0.100 $L.mg^{-1}$, respectively, LRT p = 0.0007). The fact that there is a faster inhibition of the enzyme by favipiravir in Mauritian macaques suggests that the discrepancy in drug concentration between the two groups might reduce with high doses.

Simulations with different dosing regimens. Average and residual concentrations were predicted to be lower in Mauritian macaques than in Chinese macaques in all scenarios. At day 7, the average total plasma concentration in Mauritian (resp. Chinese) cynomolgus macaques were equal to 67 (resp. 124), 215 (resp. 284) and 312 (resp. 384) mg/L for maintenance doses of 100, 150 and 180 mg/kg BID, respectively. In order to achieve similarly high concentrations in Mauritian cynomolgus macaques, maintenance dose would need to be equal to 120, 170 and 200 mg/kg BID respectively (not shown). Loading dose was found to increase concentrations on day 1 and 2, but had limited impact on enzyme inhibition afterwards (Table A1). No steady state was reached during the dosing period and concentrations were predicted to decrease over time with a fall in average concentration of 51%, 39 % and 30% between day 7 and day 14 for maintenance doses of 100, 150 and 180 mg/kg BID, respectively, in Mauritian cynomolgus macaques. Increasing the maintenance dose from 100 to 120 mg/kg BID (Chinese origin) and

from 150 to 180 mg/kg BID (Mauritian origin) on day 7 would allow to maintain concentration until day 14 (Figure 4).

Drug exposure and EC_{50} against hemorrhagic fever viruses. In Chinese cynomolgus macaques the model predicted that a maintenance dose of 100 mg/kg BID may be sufficient to maintain median trough concentrations at day 7 above the EC_{50} of all virus except EBOV and YFV (Figure 4). In order to maintain free drug concentrations above EC_{50} until day 14, the model predicted that an increase in dose at day 7 from 100 to 120 mg/kg BID is necessary. For EBOV and YFV, higher doses of 150 mg/kg BID until day 7 followed by180 mg/kg BID afterwards were predicted to maintain free concentrations above the drug EC_{50} until day 14 (Figure 4).

In Mauritian macaques the model predicted that a maintenance dose of 150 mg/kg BID may be sufficient to maintain median trough concentrations at all time above the EC_{50} of all viruses except EBOV and YFV (Figure 4, Table A1). In the case of EBOV and YFV, a maintenance dose of 180 mg/kg BID maintains the concentrations above the drug EC_{50} until day 7, but not afterwards (Figure 4).

DISCUSSION

The pharmacokinetics of favipiravir exhibited nonlinearity over dose and over time, with a marked increase in drug concentration between the first and the second administration followed by a progressive reduction afterwards until the end of the dosing period. A model with an enzyme inhibition process was developed to characterize this complex profile, which allowed us to fit the data and to make predictions for a variety of unobserved scenarios.

The complexity of the drug PK and the large variability in drug concentrations across animals is likely due to the fact that favipiravir inhibits aldehyde oxidase, which is the main enzyme involved in the drug elimination (21). This enzyme targets and is inhibited by many molecules *in vitro*, such as raloxifene, menadione or amitriptyline (27). There are no data to our knowledge on the aldehyde oxidase phenotypes across macaque populations. However it is known that Mauritian and South East Asia cynomolgus populations have a genetic gap (28, 29) and therefore it is possible that this genetic difference explains the discrepancy in PK between the two species. In spite of the efforts to standardize the protocol studies and animal handling, the experiments were performed in two different laboratories and thus one cannot rule out that differences found between the two species are due to confounding factors.

Another intriguing pattern of the drug PK was the decrease in drug concentrations over time, which was captured by using a time-varying parameter. We also tested a more physiological model with a feedback mechanism where the decrease of the aldehyde oxidase activity due to favipiravir increases enzyme synthesis but the data fitting was not improved. It is noteworthy that a decrease in drug concentrations over time was also reported in EBOV infected patients treated with high doses of favipiravir (unpublished results).

In terms of safety, a decrease in food consumption imputed to favipiravir was observed during the dosing period in the study 1B at the dose of 150 mg/kg BID leading to dosing discontinuation on day 11, but not in those of study 2B treated for 7 days with 180 mg/kg BID, which still had higher exposure (Table 2). Global impairment of psychomotor activities, including decrease in food intake, was previously reported during oral dose toxicity study in Chinese cynomolgus receiving 1000 mg/kg/day, confirming results in other species that high concentrations of favipiravir transiently depress central nervous system (Japanese Pharmaceuticals and Medical Devices Agency (PMDA) report, https://www.pmda.go.jp/files/000210319.pdf). Besides this observation, no other abnormalities in body weights, serum electrolyte concentrations, general condition or necropsy were reported in macaques which required dosing interruption. Considering the four studies, some biological alterations were noticed, in particular anemia and liver cytolysis (see supplementary material). These changes were also previously reported in toxicity studies (PMDA report, https://www.pmda.go.jp/files/000210319.pdf) and they were reversible after one month recovery.

In order to simulate the drug exposure with different dosing regimens a number of assumptions have been done. First, the studies were conducted in non-infected animals and the infection may alter the drug concentration. For instance a decrease of favipiravir concentration was observed in a hamster model of arenavirus hemorrhagic fever (30). Besides, no PK sample was performed from the tissues to explore favipiravir diffusion. Second, the criterion used to propose the dosing regimens was based on the comparison between the EC_{50} observed *in vitro* and the free plasma concentration of favipiravir, which yet may not be the best marker of nucleoside analogue antiviral activity. Indeed, the active form of favipiravir is the intracellular triphosphate metabolite (31), which could present a different kinetic from the parent form, as it was observed for other nucleoside analogues in HIV infection (32). Nonetheless the half-life of the intracellular triphosphate metabolite, as estimated in human peripheral blood mononuclear cells, is equal to 2 hours (PMDA report, https://www.pmda.go.jp/files/000210319.pdf).

Although a longer value (5.6 hr) was found in influenza infected MDCK cells (33), these values are comparable to plasma favipiravir half-life that range from 2h to 6h, as found in this study and in other contexts (21). Therefore, the PK of the active intracellular metabolite is likely limited by its rate of formation and it is reasonable to assume that the antiviral activity is driven by favipiravir PK. Third, the criterion to find relevant dosing regimens was based on the pre-dose drug concentrations but average or cumulative exposure may also be relevant. More generally, the exposure-response relationship cannot be anticipated and a PK-viral dynamic analysis, as proposed for in instance in mice infected with EBOV (34), will be needed to fully characterize the antiviral activity of favipiravir. In that respect, viral dynamic modeling teaches that the time of treatment initiation is critical to reduce viral levels, and that a drug affecting viral replication, such as favipiravir, will only have a very limited impact on viremia if it is administered after the peak viremia (34). Further, the duration of the treatment may also be critical as previous studies showed that EBOV-infected macaques treated with BCX4430 or ZMapp may still have detectable viremia 14 days post challenge (35, 36). Treatment duration and exposure can also in theory affect resistance emergence. Although there is no evidence so far of resistance to favipiravir in influenza or HF viruses (10, 37), the emergence of Chikungunya resistant mutants consecutive to a low-level exposure to favipiravir in cellular culture was reported (38). Therefore, it cannot be ruled out that treatment duration, in particular if drug concentration decline over time, may increase the risk of resistance emergence.

To conclude, we developed a mathematical model to predict the plasma exposure to favipiravir in NHPs with various dosing regimen. This information can be used to design studies evaluating favipiravir efficacy and to characterize the dose-response relationship of favipiravir against a variety of viruses responsible for HF

FUNDING INFORMATION

This project has received funding from the European Union's Horizon 2020 research and innovation program under grant agreement No. 666092, and from Saint Luke University (Japan).

Transparency declaration

This project (VM, JG, FM, THT, FJ, XdL, HR) has received funding from the European Union's Horizon 2020 research and innovation programme under grant agreement No. 666092

and from Saint Luke University (Japan). LO was supported by a grant from the European Commission to evaluate the effect of favipiravir on replication of Marburg virus in cell culture. TK and KY are employed by Toyama chemicals, manufacturer of favipiravir. AMT declared no conflict of interest.

REFERENCES

1. **Beeching NJ**, **Fenech M**, **Houlihan CF**. 2014. Ebola virus disease. BMJ **349**:g7348.

2. **van Paassen J**, **Bauer MP**, **Arbous MS**, **Visser LG**, **Schmidt-Chanasit J**, **Schilling S**, **Ölschläger S**, **Rieger T**, **Emmerich P**, **Schmetz C**, **van de Berkmortel F**, **van Hoek B**, **van Burgel ND**, **Osterhaus AD**, **Vossen AC**, **Günther S**, **van Dissel JT**. 2012. Acute liver failure, multiorgan failure, cerebral oedema, and activation of proangiogenic and antiangiogenic factors in a case of Marburg haemorrhagic fever. Lancet Infect Dis **12**:635–642.

3. **Guzman MG**, **Harris E**. 2015. Dengue. Lancet Lond Engl **385**:453–465.

4. **Grant A**, **Seregin A**, **Huang C**, **Kolokoltsova O**, **Brasier A**, **Peters C**, **Paessler S**. 2012. Junín Virus Pathogenesis and Virus Replication. Viruses **4**:2317–2339.

5. **Ergönül O**. 2006. Crimean-Congo haemorrhagic fever. Lancet Infect Dis **6**:203–214.

6. **Ikegami T**, **Makino S**. 2011. The pathogenesis of Rift Valley fever. Viruses **3**:493–519.

7. **Richmond JK**, **Baglole DJ**. 2003. Lassa fever: epidemiology, clinical features, and social consequences. BMJ **327**:1271–1275.

8. **Monath TP**, **Vasconcelos PFC**. 2015. Yellow fever. J Clin Virol Off Publ Pan Am Soc Clin Virol **64**:160–173.

9. **Pigott DC**. 2005. Hemorrhagic fever viruses. Crit Care Clin **21**:765–783, vii.

10. **Furuta Y**, **Gowen BB**, **Takahashi K**, **Shiraki K**, **Smee DF**, **Barnard DL**. 2013. Favipiravir (T-705), a novel viral RNA polymerase inhibitor. Antiviral Res **100**:446–454.

11. **Oestereich L**, **Lüdtke A**, **Wurr S**, **Rieger T**, **Muñoz-Fontela C**, **Günther S**. 2014. Successful treatment of advanced Ebola virus infection with T-705 (favipiravir) in a small animal model. Antiviral Res **105**:17–21.

12. **Oestereich L**, **Rieger T**, **Neumann M**, **Bernreuther C**, **Lehmann M**, **Krasemann S**, **Wurr S**, **Emmerich P**, **de Lamballerie X**, **Ölschläger S**, **Günther S**. 2014. Evaluation of antiviral efficacy of ribavirin, arbidol, and T-705 (favipiravir) in a mouse model for Crimean-Congo hemorrhagic fever. PLoS Negl Trop Dis **8**:e2804.

13. **Oestereich L**, **Rieger T**, **Lüdtke A**, **Ruibal P**, **Wurr S**, **Pallasch E**, **Bockholt S**, **Krasemann S**, **Muñoz-Fontela C**, **Günther S**. 2016. Efficacy of Favipiravir Alone and in Combination With Ribavirin in a Lethal, Immunocompetent Mouse Model of Lassa Fever. J Infect Dis **213**:934–938.

14. **Caroline AL**, **Powell DS**, **Bethel LM**, **Oury TD**, **Reed DS**, **Hartman AL**. 2014. Broad spectrum antiviral activity of favipiravir (T-705): protection from highly lethal inhalational Rift Valley Fever. PLoS Negl Trop Dis **8**:e2790.

15. **Safronetz D**, **Rosenke K**, **Westover JB**, **Martellaro C**, **Okumura A**, **Furuta Y**, **Geisbert J**, **Saturday G**, **Komeno T**, **Geisbert TW**, **Feldmann H**, **Gowen BB**. 2015. The broad-spectrum antiviral favipiravir protects guinea pigs from lethal Lassa virus infection post-disease onset. Sci Rep **5**:14775.

16. **Smither SJ**, **Eastaugh LS**, **Steward JA**, **Nelson M**, **Lenk RP**, **Lever MS**. 2014. Post-exposure efficacy of oral T-705 (Favipiravir) against inhalational Ebola virus infection in a mouse model. Antiviral Res **104**:153–155.

17. **Gowen BB**, **Wong M-H**, **Jung K-H**, **Sanders AB**, **Mendenhall M**, **Bailey KW**, **Furuta Y**, **Sidwell RW**. 2007. In vitro and in vivo activities of T-705 against arenavirus and bunyavirus infections. Antimicrob Agents Chemother **51**:3168–3176.

18. **Julander JG**, **Shafer K**, **Smee DF**, **Morrey JD**, **Furuta Y**. 2009. Activity of T-705 in a Hamster Model of Yellow Fever Virus Infection in Comparison with That of a Chemically Related Compound, T-1106. Antimicrob Agents Chemother **53**:202–209.

19. **Sissoko D**, **Laouenan C**, **Folkesson E**, **M'Lebing A-B**, **Beavogui A-H**, **Baize S**, **Camara A-M**, **Maes P**, **Shepherd S**, **Danel C**, **Carazo S**, **Conde MN**, **Gala J-L**, **Colin G**, **Savini H**, **Bore JA**, **Le Marcis F**, **Koundouno FR**, **Petitjean F**, **Lamah M-C**, **Diederich S**, **Tounkara A**, **Poelart G**, **Berbain E**, **Dindart J-M**, **Duraffour S**, **Lefevre A**, **Leno T**, **Peyrouset O**, **Irenge L**, **Bangoura N**, **Palich R**, **Hinzmann J**, **Kraus A**, **Barry TS**, **Berette S**, **Bongono A**, **Camara MS**, **Chanfreau Munoz V**, **Doumbouya L**, **Souley Harouna null**, **Kighoma PM**, **Koundouno FR**, **Réné Lolamou null**, **Loua CM**, **Massala V**, **Moumouni K**, **Provost C**, **Samake N**, **Sekou C**, **Soumah A**, **Arnould I**, **Komano MS**, **Gustin L**, **Berutto C**, **Camara D**, **Camara FS**, **Colpaert J**, **Delamou L**, **Jansson L**, **Kourouma E**, **Loua M**, **Malme K**, **Manfrin E**, **Maomou A**, **Milinouno A**, **Ombelet S**, **Sidiboun AY**, **Verreckt I**, **Yombouno P**, **Bocquin A**, **Carbonnelle C**, **Carmoi T**, **Frange P**, **Mely S**, **Nguyen V-K**, **Pannetier D**, **Taburet A-M**, **Treluyer J-M**, **Kolie J**, **Moh R**, **Gonzalez MC**, **Kuisma E**, **Liedigk B**, **Ngabo D**, **Rudolf M**, **Thom R**, **Kerber R**, **Gabriel M**, **Di Caro A**, **Wölfel R**, **Badir J**, **Bentahir M**, **Deccache Y**, **Dumont C**, **Durant J-F**, **El Bakkouri K**, **Gasasira Uwamahoro M**,

Smits B, **Toufik N**, **Van Cauwenberghe S**, **Ezzedine K**, **Dortenzio E**, **Pizarro L**, **Etienne A**, **Guedj J**, **Fizet A**, **Barte de Sainte Fare E**, **Murgue B**, **Tran-Minh T**, **Rapp C**, **Piguet P**, **Poncin M**, **Draguez B**, **Allaford Duverger T**, **Barbe S**, **Baret G**, **Defourny I**, **Carroll M**, **Raoul H**, **Augier A**, **Eholie SP**, **Yazdanpanah Y**, **Levy-Marchal C**, **Antierrens A**, **Van Herp M**, **Günther S**, **de Lamballerie X**, **Keïta S**, **Mentre F**, **Anglaret X**, **Malvy D**, **JIKI Study Group**. 2016. Experimental Treatment with Favipiravir for Ebola Virus Disease (the JIKI Trial): A Historically Controlled, Single-Arm Proof-of-Concept Trial in Guinea. PLoS Med **13**:e1001967.

20. **Shurtleff AC**, **Warren TK**, **Bavari S**. 2011. Nonhuman primates as models for the discovery and development of ebolavirus therapeutics. Expert Opin Drug Discov **6**:233–250.

21. **Madelain V**, **Nguyen THT**, **Olivo A**, **de Lamballerie X**, **Guedj J**, **Taburet A-M**, **Mentré F**. 2016. Ebola Virus Infection: Review of the Pharmacokinetic and Pharmacodynamic Properties of Drugs Considered for Testing in Human Efficacy Trials. Clin Pharmacokinet **55**:907–923.

22. **Lavielle M**. 2014. Using Models, p. 161–197. *In* Mixed Effects Models for the Population Approach: Models, Tasks, Methods and Tools. CRC Press.

23. **Samson A**, **Lavielle M**, **Mentré F**. 2006. Extension of the SAEM algorithm to left-censored data in nonlinear mixed-effects model: Application to HIV dynamics model. Comput Stat Data Anal **51**:1562–1574.

24. **Bergstrand M**, **Hooker AC**, **Wallin JE**, **Karlsson MO**. 2011. Prediction-corrected visual predictive checks for diagnosing nonlinear mixed-effects models. AAPS J **13**:143–151.

461 25. **Comets E**, **Brendel K**, **Mentré F**. 2010. Model evaluation in nonlinear mixed effect
462 models, with applications to pharmacokinetics. J Société Fr Stat **151**:106–128.

463 26. **Mentré F**, **Taburet A-M**, **Guedj J**, **Anglaret X**, **Keïta S**, **de Lamballerie X**, **Malvy D**.
464 2015. Dose regimen of favipiravir for Ebola virus disease. Lancet Infect Dis **15**:150–
465 151.

466 27. **Obach RS**, **Huynh P**, **Allen MC**, **Beedham C**. 2004. Human liver aldehyde oxidase:
467 inhibition by 239 drugs. J Clin Pharmacol **44**:7–19.

468 28. **Tosi AJ**, **Coke CS**. 2007. Comparative phylogenetics offer new insights into the
469 biogeographic history of Macaca fascicularis and the origin of the Mauritian macaques.
470 Mol Phylogenet Evol **42**:498–504.

471 29. **Ogawa LM**, **Vallender EJ**. 2014. Genetic substructure in cynomolgus macaques
472 (Macaca fascicularis) on the island of Mauritius. BMC Genomics **15**:748.

473 30. **Gowen BB**, **Sefing EJ**, **Westover JB**, **Smee DF**, **Hagloch J**, **Furuta Y**, **Hall JO**. 2015.
474 Alterations in favipiravir (T-705) pharmacokinetics and biodistribution in a hamster
475 model of viral hemorrhagic fever. Antiviral Res **121**:132–137.

476 31. **Furuta Y**, **Takahashi K**, **Kuno-Maekawa M**, **Sangawa H**, **Uehara S**, **Kozaki K**,
477 **Nomura N**, **Egawa H**, **Shiraki K**. 2005. Mechanism of action of T-705 against
478 influenza virus. Antimicrob Agents Chemother **49**:981–986.

479 32. **Bazzoli C**, **Jullien V**, **Le Tiec C**, **Rey E**, **Mentré F**, **Taburet A-M**. 2010. Intracellular
480 Pharmacokinetics of Antiretroviral Drugs in HIV-Infected Patients, and their Correlation
481 with Drug Action. Clin Pharmacokinet **49**:17–45.

33. **Smee DF**, **Hurst BL**, **Egawa H**, **Takahashi K**, **Kadota T**, **Furuta Y**. 2009. Intracellular metabolism of favipiravir (T-705) in uninfected and influenza A (H5N1) virus-infected cells. J Antimicrob Chemother **64**:741–746.

34. **Madelain V**, **Oestereich L**, **Graw F**, **Nguyen THT**, **de Lamballerie X**, **Mentré F**, **Günther S**, **Guedj J**. 2015. Ebola virus dynamics in mice treated with favipiravir. Antiviral Res **123**:70–77.

35. **Warren TK**, **Wells J**, **Panchal RG**, **Stuthman KS**, **Garza NL**, **Van Tongeren SA**, **Dong L**, **Retterer CJ**, **Eaton BP**, **Pegoraro G**, **Honnold S**, **Bantia S**, **Kotian P**, **Chen X**, **Taubenheim BR**, **Welch LS**, **Minning DM**, **Babu YS**, **Sheridan WP**, **Bavari S**. 2014. Protection against filovirus diseases by a novel broad-spectrum nucleoside analogue BCX4430. Nature **508**:402–405.

36. **Qiu X**, **Wong G**, **Audet J**, **Bello A**, **Fernando L**, **Alimonti JB**, **Fausther-Bovendo H**, **Wei H**, **Aviles J**, **Hiatt E**, **Johnson A**, **Morton J**, **Swope K**, **Bohorov O**, **Bohorova N**, **Goodman C**, **Kim D**, **Pauly MH**, **Velasco J**, **Pettitt J**, **Olinger GG**, **Whaley K**, **Xu B**, **Strong JE**, **Zeitlin L**, **Kobinger GP**. 2014. Reversion of advanced Ebola virus disease in nonhuman primates with ZMapp. Nature **514**:47–53.

37. **Takashita E**, **Ejima M**, **Ogawa R**, **Fujisaki S**, **Neumann G**, **Furuta Y**, **Kawaoka Y**, **Tashiro M**, **Odagiri T**. 2016. Antiviral susceptibility of influenza viruses isolated from patients pre- and post-administration of favipiravir. Antiviral Res **132**:170–177.

38. **Delang L**, **Segura Guerrero N**, **Tas A**, **Quérat G**, **Pastorino B**, **Froeyen M**, **Dallmeier K**, **Jochmans D**, **Herdewijn P**, **Bello F**, **Snijder EJ**, **de Lamballerie X**, **Martina B**, **Neyts J**, **van Hemert MJ**, **Leyssen P**. 2014. Mutations in the chikungunya

virus non-structural proteins cause resistance to favipiravir (T-705), a broad-spectrum antiviral. J Antimicrob Chemother **69**:2770–2784.

511 ***Tables***

512

513 *Table 1: In vitro favipiravir antiviral activity against several hemorrhagic fever viruses obtained by virus titer reduction assays on Vero cells.*

Virus	***Strain***	***EC_{50} (µg/mL)***	***EC_{90} (µg/mL)***	***References***
MARV	*Leiden*	*6.8*	*11.4*	*(Supplementary material)*
RVFV	*MP-12*	*5*	*ND*	*(17)*
JUNV	*Candid 1*	*0.79*	*ND*	*(17)*
JUNV	*Romero*	*1.9*	*3.3*	*(17)*
LASV	*Ba366*	*4.6*	*6.8*	*(13)*
LASV	*Josiah*	*1.7-11.1*	*1.7-11.1*	*(15)*
CCHFV	*Afg-09 2990*	*1.1*	*1.2-4.7*	*(12)*
EBOV	*Mayinga 1976*	*10.5*	*17.3*	*(11)*
EBOV	*Kikwit 1995/E718*	*31-63*	*31-63*	*(16)*
YFV	*17D*	*42.4*	*51.8*	*(18)*

ND: not determined

514

515

Table 2: Non compartmental analysis of favipiravir pharmacokinetic studies in cynomolgus macaques. Median [min-max] of each parameters were reported for the different studies. Study 1A: Non anesthetized Male Chinese Cynomolgus treated for 7 days; Study 1B: Anesthetized Female Chinese Cynomolgus treated for 14 days; Study 2A: Anesthetized Female Mauritian Cynomolgus treated for 14 days; Study 2B: Anesthetized Female Mauritian Cynomolgus treated for 7 days. BLQ data below the limit of quantification.

Study	Number of animals	Loading dose (mg/kg BID)	Maintenance dose (mg/kg BID)	C_{trough} (mg/L) Median (min-max)			C_{max} (mg/L) Median (min-max)			C_{ave} (mg/L) Median (min-max)			CL (L/h/kg) Median (min-max)		
				D1	D7	D14	D1	D7	D14	D1	D7	D14	D1	D7	D14
1A	**n=3**	**300**	**150**	76.5 [51.2-120.0]	97.4 [61.8-231.0]	ND	482.0 [472-597]	425 [415-593]	ND	244.1 [222.2-263.2]	240.7 [210.6-358.2]	ND	0.10 [0.10-0.11]	0.05 [0.03-0.06]	ND
	n=3	**300**	**100**	58.6 [32.9-175.0]	24.3 [2.8-35.5]	ND	520 [508-653]	265.0 [229.0-288.0]	ND	223.1 [187.9-351.3]	110.9 [61.1-117.8]	ND	0.11 [0.07-0.13]	0.08 [0.07-0.14]	ND
	n=3	**300**	**60**	98.9 [51.1-127.0]	BLQ [BLQ-15.7]	ND	408.0 [327.0-575.0]	115.0 [106.0-165.0]	ND	203.5 [189.9-309.9]	23.6 [18.0-73.9]	ND	0.12 [0.08-0.13]	0.22 [0.07-0.28]	ND
1B	**n=4**	**250**	**150**	31.2 [0.5-99.3]	105.6 [68.4-178.0]	56.8* [34.2-130.0]	545.0 [531.0-642.0]	509.5 [467.0-590.0]	470.5* [368.0-506.0]	88.4 [54.3-117.7]	241.4 [214.0-347.6]	194.3* [167.3-283.8]	0.25 [0.18-0.38]	0.03 [0.02-0.04]	0.04* [0.03-0.05]
	n=4	**200**	**100**	3.3 [0.6-5.5]	30.9 [17.8-52.8]	11.6 [7.1-32.9]	473.5 [362.0-539.0]	328.5 [310.0-370.0]	289.5 [271.0-317.0]	60.3 [51.0-72.9]	131.6 [107.5-159.0]	102.2 [85.3-133.2]	0.28 [0.23-0.33]	0.06 [0.05-0.08]	0.09 [0.06-0.10]
2A	**n=5**	**200**	**100**	BLQ [BLQ-5.8]	9.7 [BLQ-18.1]	10.3 [BLQ-37.3]	316.2 [227.9-378.9]	274.8 [133.2-354.0]	291.4 [175.4-339.2]	40.1 [20.9-63.0]	ND	47.9 [16.9-89.9]	0.42 [0.26-0.80]	ND	0.17 [0.09-0.49]
2B	**n=4**	**250**	**180**	10.4 [BLQ-35.9]	138.8 [85.4-397.8]	ND	546.1 [515.8-692.1]	829.2 [683.0-898.7]	ND	ND	368.3 [263.3-626.7]	ND	ND	0.04 [0.02-0.06]	ND
	n=4	**250**	**150**	BLQ [BLQ-8.4]	46.0 [21.8-70.5]	ND	481.8 [449.8-573.7]	445.9 [337.8-491.9]	ND	ND	187.1 [150.6-217.8]	ND	ND	0.07 [0.06-0.08]	ND

**Non-compartmental parameters calculated at day 11 due to premature dosing interruption; ND: not determined*

522 *Table 3: Pharmacokinetic model parameter estimates and associated relative standard errors.*

Fixed effect	***Fixed effects Estimates (RSE,%)***	***Interindividual variability ω (%) (RSE, %)***
V_d ***(L/kg)***	*0.359 (2.8%)*	*13.9% (14.5%)*
k (h^{-1})	*0.0654 (6.6%)*	*23.4% (15.2%)*
k_{enz} ***Mauritian origin*** (h^{-1})	*2.85 (9.8%)*	*24.2% (13.0%)*
k_{enz} ***Chinese origin*** (h^{-1})	*1.25 (8.8%)*	
α_{deg} ***Mauritian origin*** $(mg^{-1}.L)$	*0.179 (10.1%)*	*0% (fixed)*
α_{deg} ***Chinese origin*** $(mg^{-1}.L)$	*0.100 (9.5%)*	
k_{out} ***Male*** (h^{-1})	*0.036 (6.4%)*	*0% (fixed)*
k_{out} ***Female*** (h^{-1})	*0.024 (6.0%)*	
λ (h^{-1})	*0.00155 (18.7%)*	*104.1% (16.3%)*
Residual error	***Estimation (rse)***	
additive (mg/L)	*2.77 (7.9%)*	
proportional	*0.155 (3.1%)*	

523

524

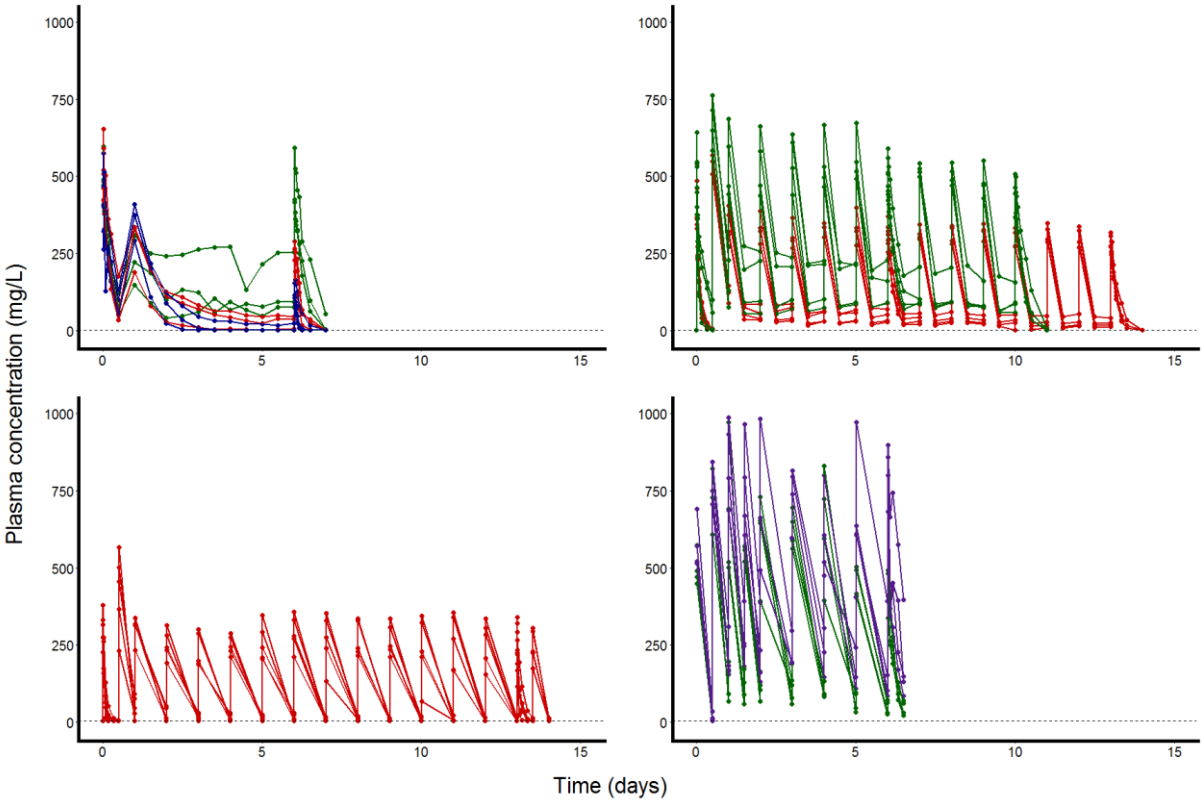

Figure 1: Individual observed pharmacokinetic profiles of favipiravir from study 1A (top left), study 1B (top right), study 2A (bottom left) and study 2B (bottom right). Study 1A: Non anesthetized Male Chinese Cynomolgus treated for 7 days; Study 1B: Anesthetized Female Chinese Cynomolgus treated for 14 days; Study 2A: Anesthetized Female Mauritian Cynomolgus treated for 14 days; Study 2B: Anesthetized Female Mauritian Cynomolgus treated for 7 days. Pharmacokinetic profile from macaques receiving maintenance dose of 60 mg/kg BID are represented in blue, 100 mg/kg BID in red, 150 mg/kg BID in green and 180 mg/kg BID in purple. Dashed line represents limit of quantification.

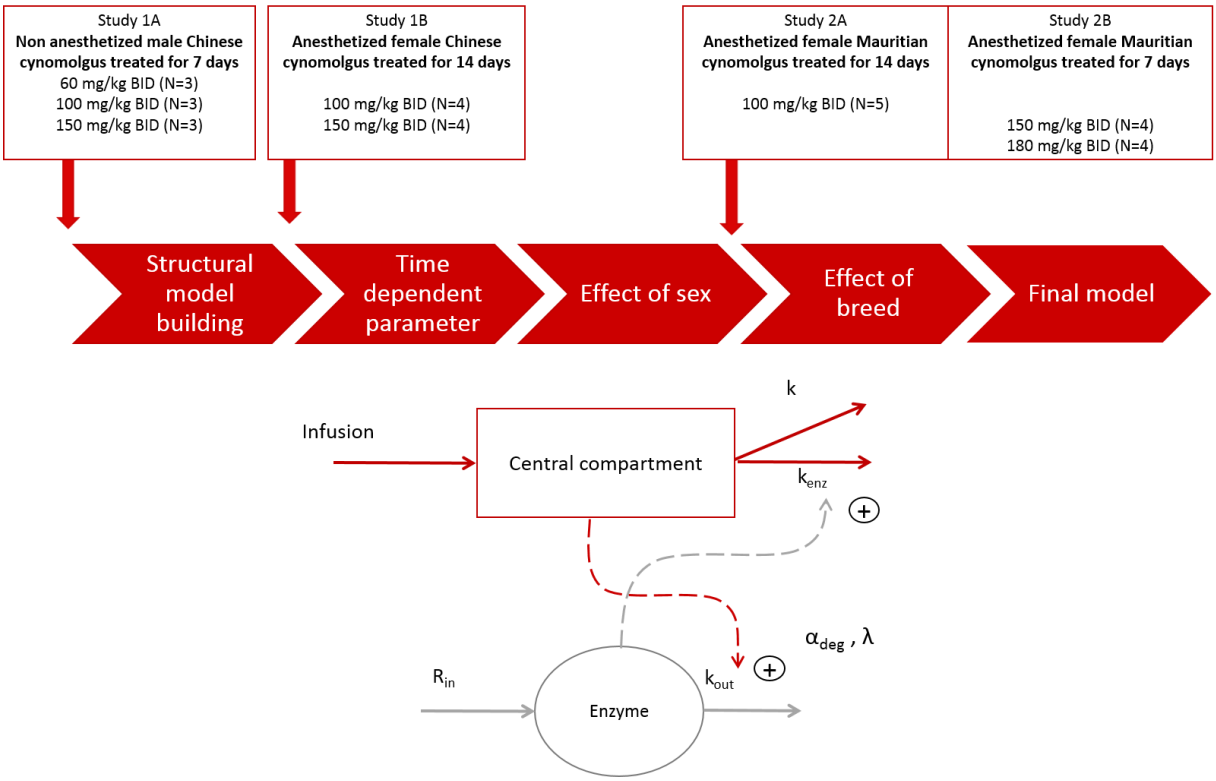

535

536

537 *Figure 2: Strategy used to build the pharmacokinetic model (top), and final pharmacokinetic*
538 *model of favipiravir in cynomolgus macaques (bottom). Parameter k is the enzyme*
539 *independent elimination rate constant, k_{enz} is the enzyme dependent elimination rate, R_{in} is the*
540 *0-order enzyme synthesis rate, k_{out} is the 1-order elimination rate, and α_{deg} is the linear effect*
541 *of favipiravir concentration on enzyme elimination constant. Parameter α_{deg} decreased*
542 *exponentially over time with a rate λ.*

543

544

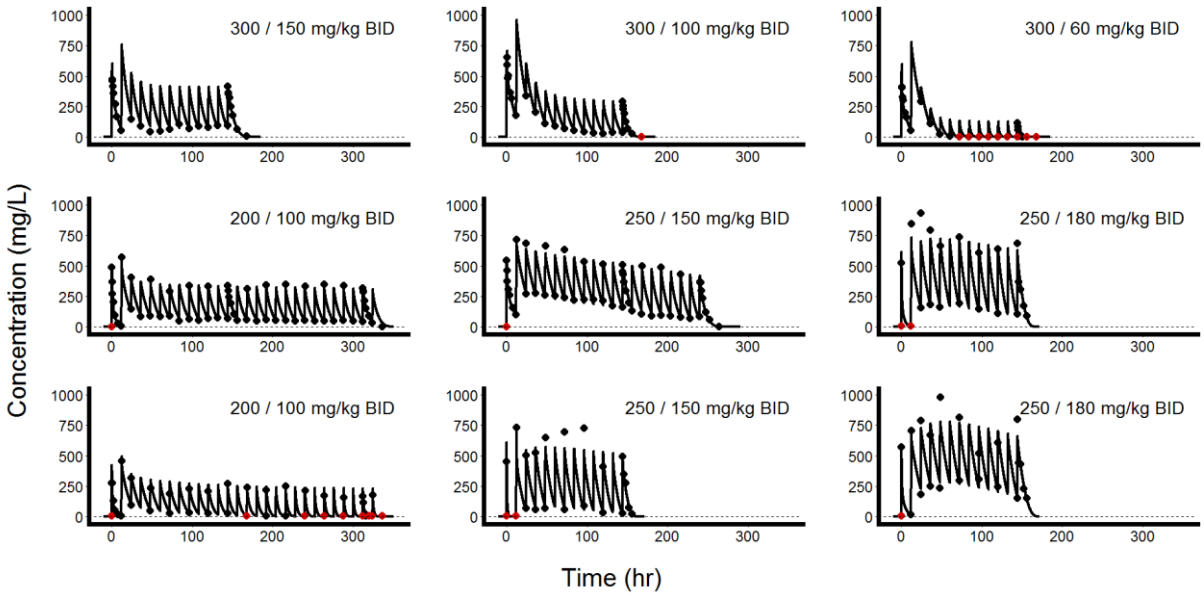

545

546 *<u>Figure 3</u>: Individual observed concentrations (black dots) and model predictions (solid line)*
547 *for macaques treated with various dosing regimens. Red dots indicate data under the limit of*
548 *quantitation, represented with a dashed line.*

549

550

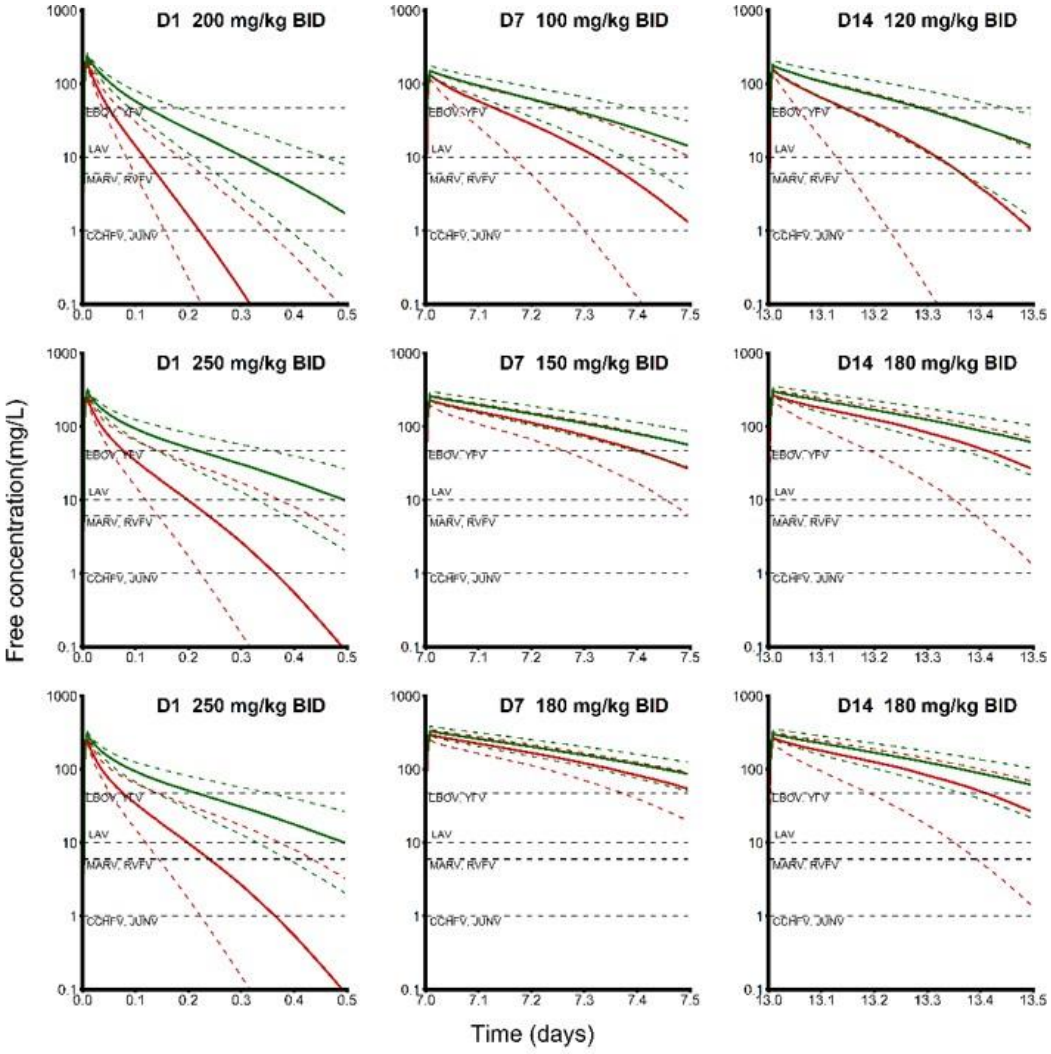

551

552 *Figure 4: Prediction of plasma free concentration (assuming a protein binding rate of 50%)*
553 *of favipiravir in female Chinese (green) and Mauritian (red) cynomolgus, on day 1 (left*
554 *panel), day 7 (middle panel) and day 14 (right panel) with various dosing regimen. Top line:*
555 *200 mg/kg BID on day 1, 100 mg/kg BID on day 2-7, 120 mg/kg on day 8-14; Middle line:*
556 *250 mg/kg BID on day 1, 150 mg/kg BID on day 2-7, 180 mg/kg on day 8-14; Bottom line:*
557 *250 mg/kg BID on day 1, 180 mg/kg BID on day 2-14. For each profile, 1000 macaques were*
558 *simulated, and median (solid line), 25th and 75th percentiles (dashed lines) were given, EC_{50}*
559 *are given in Table 1. EBOV: Ebola virus; YFV: Yellow fever virus; LAV: Lassa fever virus;*
560 *MARV: Marburg virus; RVFV: Rift valley fever virus; CCHFV: Crimea-Congo hemorragic*
561 *fever virus; JUNV: Junin virus*

562

563

564

565

566

Supplementary material:

Macaque handling:

In studies 1A and 1B, cynomolgus macaques (*Macaca fascicularis*) from China were provided by Charles River Laboratories Japan, Inc., and were quarantined and acclimated for 6 weeks or more at the test facility. Macaques were kept in individual cages, with temperature range of 24 – 27 °C and lightening period of 12 hours per day. Diet (pellets, high calorie liquid and fruit) was given daily, water was delivered throughout the day with automatic system. Macaques were assigned to the test groups three days before initial dosing by weight-stratified randomization.

In studies 2A and 2B, cynomolgus macaques (*Macaca fascicularis*) from Mauritius were provided by LCL-Cynologics (Port-Louis, Mauritius), and were quarantined and acclimated for 1 weeks at the test facility. Macaques were kept in individual cages, with temperature range of 23 – 24°C and lightening period of 12 hours per day in study 2A and 14.5 hours per day in study 2B. Diet (pellets, fruit) was given daily, water was available throughout the day. Macaques were assigned to the test groups using body weights before initial dosing by weight-stratified randomization.

Safety:

Several adverse events were reported consecutively to favipiravir administration in the four studies, yet none of them was considered as serious abnormality. Vomiting was the most common, systematically occurred within 4 days after treatment initiation, and was reported once in 3 animals in study 1A, once in 5 animals in study 1B, once in one animal in study 2A and once to thrice in 5 animals in study 2B. Transient absence of stool lasting 1 or 2 days, excepted for one animal (4 days), was observed in 3 animals in study 1B and 6 animals in study 2B. Stereotypies, described as intermittent backward head movements, were reported only in studies 2A and 2B, respectively in one and two animals.

Food consumption had large intra and inter individual variability along the studies (Figure A1). Transient decrease of food consumption was observed in the four studies within the 3 days after treatment initiation, followed with clear rebound, excepted in the study 1B group receiving 150 mg/kg BID. In this last group, food intake remains irregular after D3. After premature dosing interruption, food intake quickly increased in 3 of 4 monkeys.

Median loss of weight along the experimentation were 0.10, 0.30, 0.32 and 0.27 kg in studies 1A, 1B, 2A and 2B respectively. No significant difference was found between the studies (Kruskal-Wallis test, $p=0.54$), the levels of maintenance dose (Kruskal-Wallis test, $p=0.87$) and the duration of the study (Wilcoxon test, $p=0.73$).

Median drop of hemoglobin blood level was found to 2.3, 2.3, 2 and 1.3 g/dL respectively in studies 1A, 1B, 2A and 2B. No significant difference was found between the studies (Kruskal-Wallis test, $p=0.75$), the levels of maintenance dose (Kruskal-Wallis test, $p=0.75$) and the duration of the study (Wilcoxon test, $p=0.12$).

Considering blood chemistry parameters, moderate increase of ALT activity, biomarker of hepatocyte cytolysis was observed in the four studies, to 38, 25, 32 and 26 IU/L. No significant difference was found between the studies (Kruskal-Wallis test, p=0.16), the levels of maintenance dose (Kruskal-Wallis test, p=0.68) and the duration of the study (Wilcoxon test, p=0.21). Plasma creatinine, biomarker of renal function, had a median increase of 18.3 µmol/L in study 2A, whereas decrease was found in study 1A (-16.8 µmol/L). Changes were low in studies 1B and 2B, +8.8 and +1.5 µmol/L respectively. These interstudies discrepancies were statically significant (Kruskal-Wallis test, p=0.003). Study duration effect was found significant (Wilcoxon test, p=0.013), pointing out a possible time related impact of favipiravir administration on renal function. Yet, the clinical impact of the observed increase remains moderate, and the statistical effect is strengthened by the creatinine decrease in study 1A. No other clinically relevant changes of blood chemistry parameters were reported.

No abnormalities were noticed in animal necropsies in studies 1B, 2A and 2B.

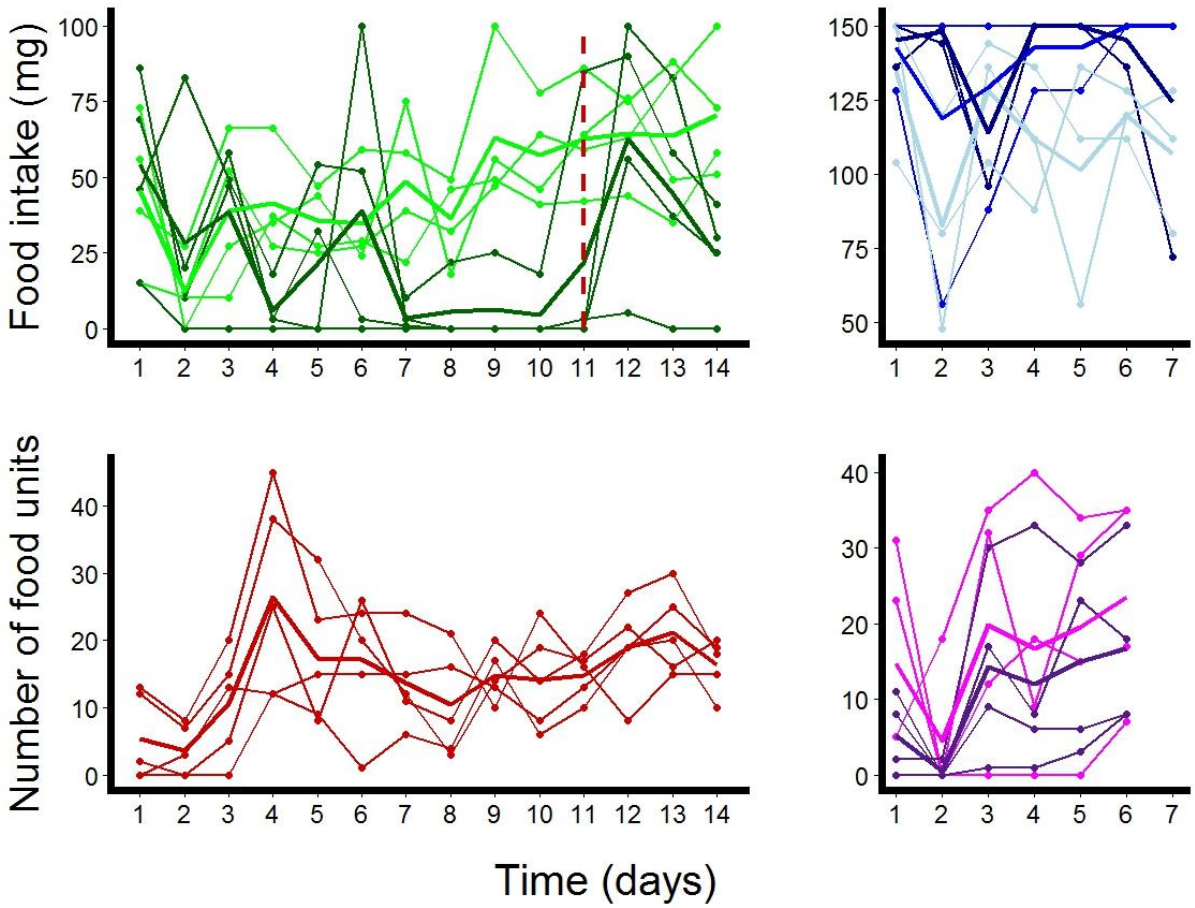

Figure A1: Food consumption evolution over study periods. Top left study 1B, light green lines 100 mg/kg group, dark green lines 150 mg/kg group, vertical red dashed line dosing interruption for 150 mg/kg. Top right study 1A, light blue lines 60 mg/kg group, blue lines 100 mg/kg group,

dark blue lines 150 mg/kg group. Bottom left study 2A, red lines 100 mg/kg group. Bottom right study 2B, magenta lines 150 mg/kg group, purple lines 180 mg/kg group. Bold solid line in each plot represent group median.

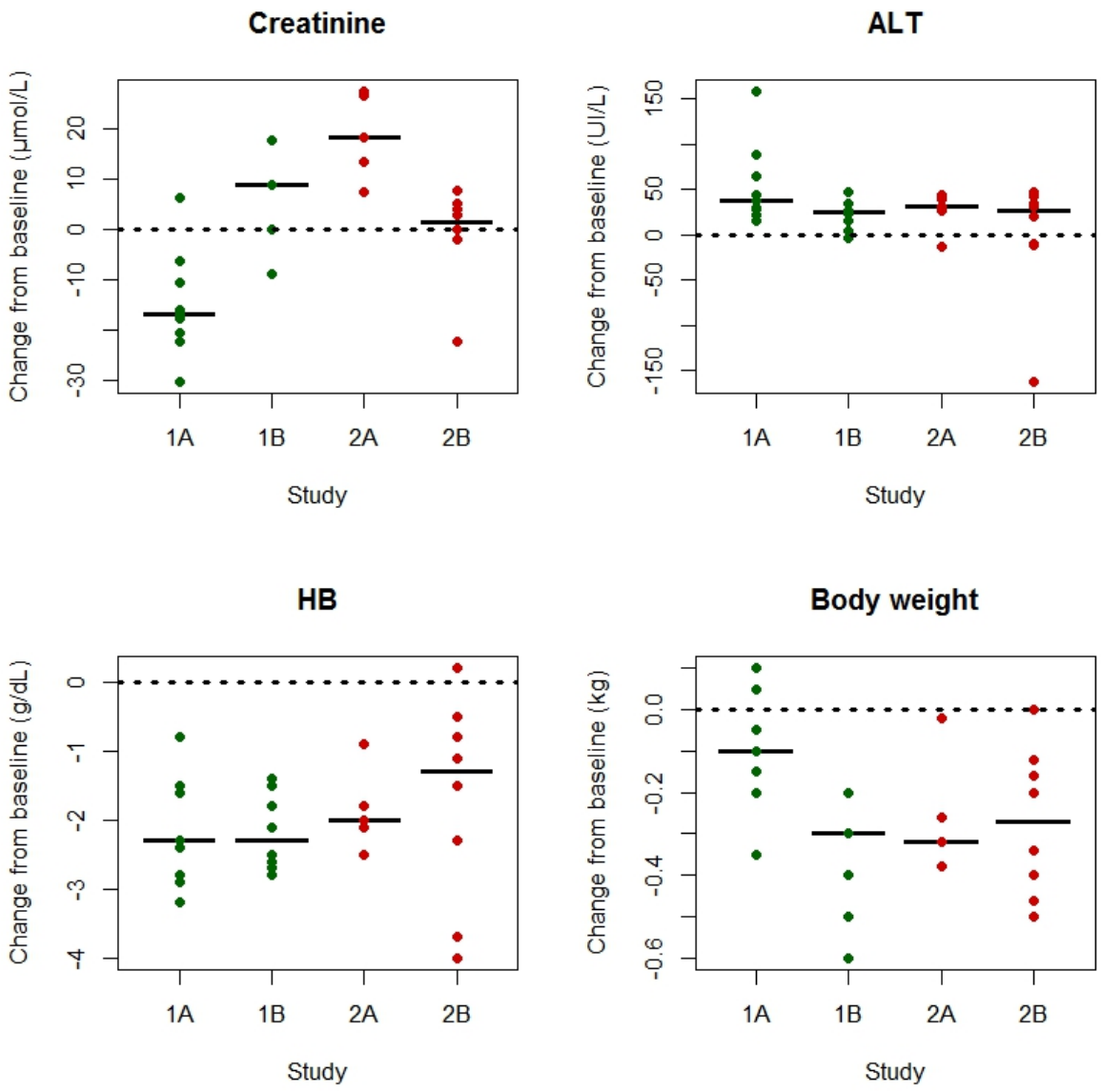

Figure A2: Clinical and biological parameters changes from baseline to end of studies. Green Chinese cynomolgus macaques, red Mauritian cynomolgus macaques.

Non compartmental analysis of favipiravir concentrations:

The maximal concentrations, C_{max} was measured 5 min after the end of the infusion and the residual concentrations, C_{trough}, was measured just before the beginning of the second infusion of the day. We considered steady state was reached at day 6. The terminal half-lives (HL) were approximated by linear regression of logarithm concentrations of the 3 final points before new administration. Areas under curve (AUC) were computed using trapezoidal method with natural concentrations. We computed $AUC_{0\text{-}12h}$ for the first dose on day 1 and last doses on day 7-14, and AUC extrapolated to infinity (AUC_{inf}) on day 1, equal to $AUC_{012} + \frac{HL \times C_{12h}}{\ln(2)}$. The average concentrations, C_{ave}, were calculated as $AUC_{0\text{-}12h}/12$. Non compartmental clearance, CL, on day 1 and days 7-14 were calculated as $CL = Dose/AUC_{inf}$ and $CL = Dose/AUC_{0\text{-}12h}$, respectively. Data below the limit of quantification were set at the limit of quantification value for the non-compartmental analysis. The analysis was performed using R software version 3.1.2.

Analysis Methods and cross validation of favipiravir concentration assay:

Methods:

Blood samples of 0.8-1.5 mL were collected in cynomolgus macaques on EDTA K2 tubes for each time point, and centrifuged in the hour following the sampling.

Analytical methods for Japanese and French studies were performed separately. Favipiravir plasma concentrations from studies 1 were assayed using reference method developed by Toyama Chemicals, Japan, called method A below, consisting in high performance liquid chromatography (HPLC) associated to UV detection (Shimadzu 10A coupled to SPD-10A, Shimadzu Corporation). The limit of quantitation of the method was 0.1 mg/L. Samples from studies 2 were assayed by Eurofin/ADME Bioanalyses, Strasbourg, France, using HPLC (Kromasil C18) coupled to tandem mass spectrometry detection (API4000), designed as method B, with a limit of quantitation of 5 mg/L.

In order to allow comparison of Chinese and Mauritian cynomolgus macaques, assessment of reproducibility of favipiravir plasma concentration analytical process was evaluated in a cross validation study. Fifteen samples of cynomolgus macaques from study 2A, 9 peaks and 6 residuals, were blindly assayed by the two laboratories. Assessment of the agreement of the two analytical processes was performed using method B concentrations vs method A concentrations

plot, differences against method A concentrations plot, and computing absolute error and relative error for each sample, as:

Error = Method B concentration – Method A concentration

Relative error = (Method B concentration – Method A concentration)/ Method A concentration

Mean, median, maximum, minimum and standard deviation of errors and relative errors were calculated. Bias and relative bias were defined as mean of error and relative error, respectively. Data below the limit of quantitation (LOQ) of Reaction's analytical process (5 mg/L) were excluded from the analysis and reported separately.

Results:

N=13	error (mg/L)	relative error
mean	-5.48	-1.1%
sd	15.59	10.1%
min	-35.16	-15.1%
max	26.35	19.8%
median	-3.60	-3.9%

Agreement between the two assays was stated by the cross validation study. Method B slightly under-predicts peak concentrations of favipiravir, and over predicts residual concentrations (Figures A3 and A4). However, only two absolute relative errors were higher than 15%, one is positive and the second negative, and the relative bias was computed to -1.1%, so is quite low. Two residual concentrations were found under the LOQ (5 mg/L) by method B, and these samples were assayed to 2.22 and 2.62 mg/L by method A, showing good agreement for the lowest concentrations.

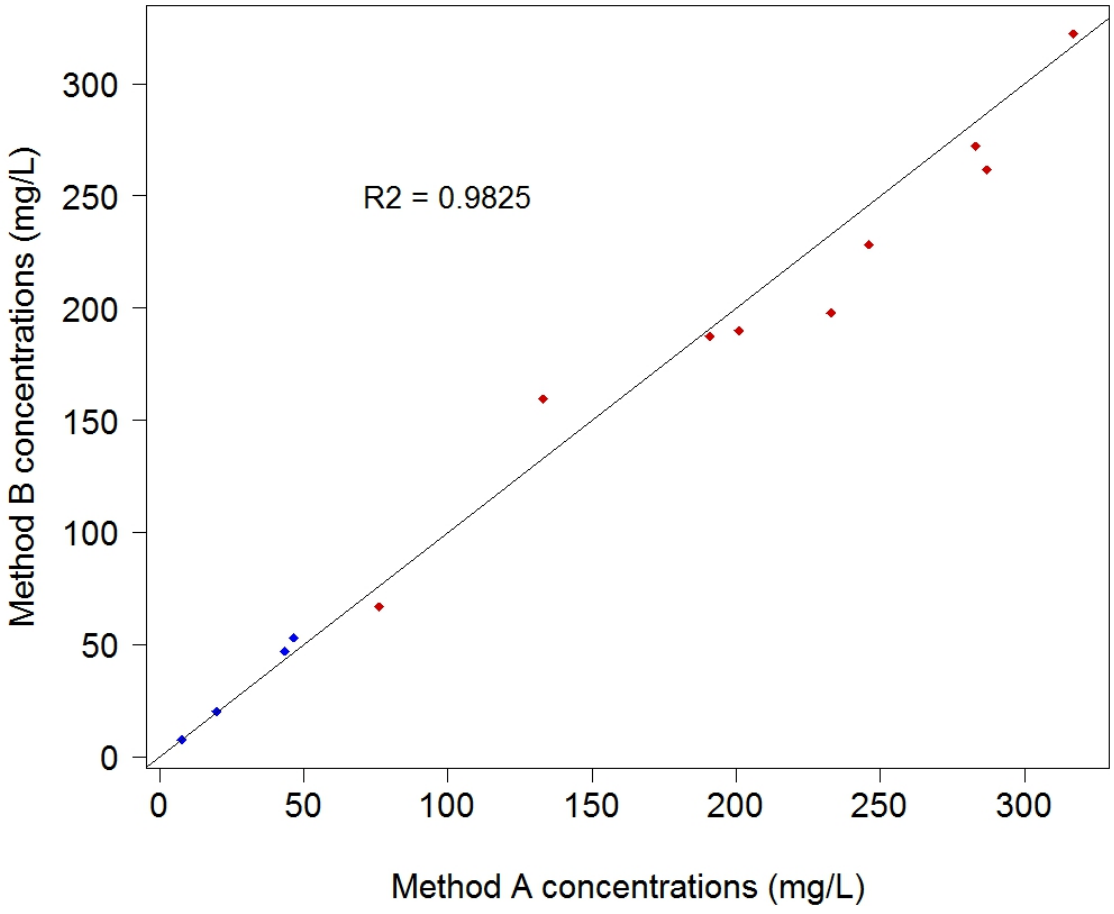

681

682 Figure A3: Favipiravir natural concentrations assayed by method B plotted vs ones assayed by
683 method A. Red dots are peak concentrations, blue ones are residual concentrations.

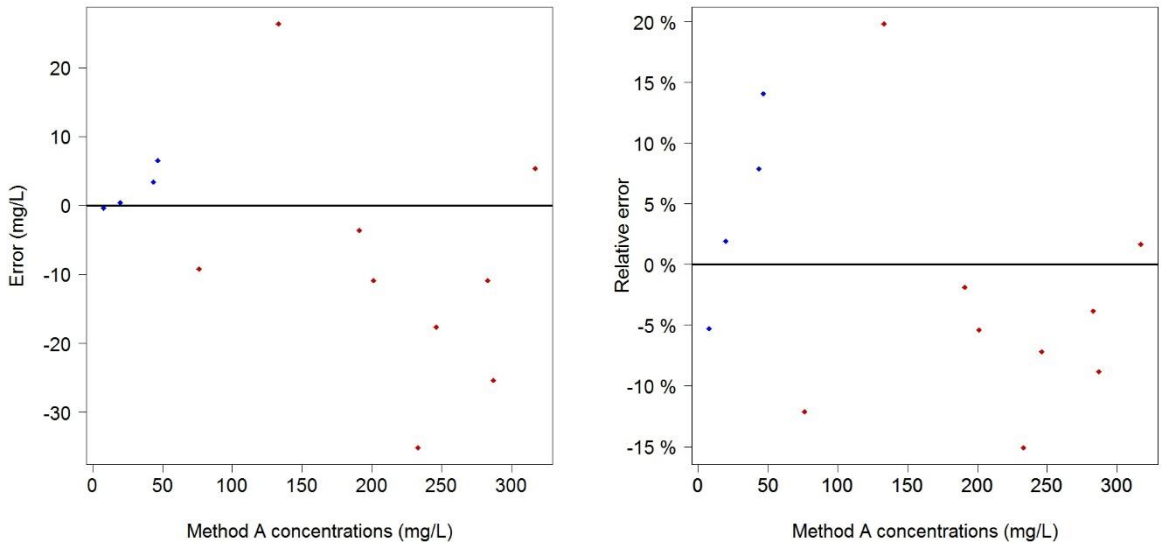

684

685 Figure A4: Error and relative errors of favipiravir concentrations plotted versus method A
686 concentrations. Red dots are peak concentrations, blue ones are residual concentrations.

Favipiravir *in vitro* EC_{50} assessment for Marburg virus

Because it was not reported in the literature, an experiment was performed to determine the EC_{50} of favipiravir against Marburg virus in the biosafety level 4 (BSL-4) laboratory at the Bernhard Nocht Institute for Tropical Medicine in Hamburg. Methodology was previously described in (12, 13). In brief, Vero E6 cells (4×10^4 cells per well) were inoculated with MARV strain Leiden (2) with a multiplicity of infection of 0.01 and drug was added 1 h post infection. Concentration in cell culture supernatant of infectious virus particles was measured 5 days post infection by real time PCR. The concentrations that reduced the virus titer by 50% and 90% (EC_{50} and EC_{90}, respectively) were calculated from dose– response curves by nonlinear regression.

Table A1: Model prediction of favipiravir plasmatic total concentration profiles in female Chinese and Mauritian cynomolgus, on day 1, day 7 and day 14 after treatment initiation. Five thousand individual profiles were simulated for each scenario, and median, 5th and 95th percentiles were reported.

Origin	Dosing (mg/kg BID)			C_{trough}(mg/L)			C_{max} (mg/L)			C_{ave} (mg/L)		
	D1	D2-D7	D8-D14	D1	D7	D14	D1	D7	D14	D1	D7	D14
Mauritian	200	60	60	0.0 [0.0-43.0]	0.0 [0.0 - 3.6]	0.0 [0.0 - 0.6]	413.0 [308.8 - 531.8]	142.4 [107.0 - 183.2]	136.0 [101.6 - 176.4]	30.6 [13.6 - 136.8]	12.8 [5.4 - 46.8]	9.0 [4.2 - 31.8]
Mauritian	100	100	100	0.0 [0.0-0.0]	3.4 [0.0 - 72.6]	0.0 [0.0 - 50.0]	200.8 [154.8 - 247.8]	265.4 [193.4 - 374.8]	246.4 [182.6 - 345.8]	9.8 [6.0 - 16.8]	67.2 [12.6 - 184.6]	33.0 [0.0 - 157.0]
Mauritian	200	100	100	0.0 [0.0 - 43.0]	3.0 [0.0 - 71.6]	0.0 [0.0 - 49.8]	413.0 [308.8 - 531.8]	264.2 [194.2 - 371.8]	246.4 [0.0 - 345.8]	30.6 [13.6 - 136.8]	67.6 [13.2 - 184.8]	33.0 [8.2 - 157.0]
Mauritian	200	100	120	0.0 [0.0 - 43.0]	3.0 [0.0 - 71.6]	1.6 [0.0 - 97.8]	413.0 [308.8 - 531.8]	264.2 [194.2 - 371.8]	306.8 [227.4 - 479.0]	30.6 [13.6 - 136.8]	67.6 [13.2 - 184.8]	59.8 [11.0 - 244.0]
Mauritian	200	100	150	0.0 [0.0 - 43.0]	3.0 [0.0 - 71.6]	15.6 [0.0 - 199.0]	413.0 [308.8 - 531.8]	264.2 [194.2 - 371.8]	406.8 [291.2 - 689.8]	30.6 [13.6 - 136.8]	67.6 [13.2 - 184.8]	125.0 [15.2 - 393.6]
Mauritian	250	130	130	0.2 [0.0 - 102.6]	31.0 [0.0 - 165.8]	4.6 [0.0 - 127.4]	520.4 [389.6 - 670.4]	379.0 [265.2 - 559.8]	339.0 [245.0 - 518.2]	53.4 [19.0 - 237.2]	149.2 [25.6 - 330.2]	81.8 [12.2 - 287.2]
Mauritian	150	150	150	0.0 [0.0 - 0.2]	60.2 [0.0 - 225.3]	16.8 [0.0 - 188.8]	304.0 [233.8 - 375.2]	459.3 [317.8 - 686.7]	408.8 [287.6 - 640.8]	17.2 [9.8 - 33.8]	215.0 [39.3 - 423.0]	132.0 [15.2 - 380.4]
Mauritian	250	150	150	0.2 [0.0 - 102.6]	60.6 [0.0 - 225.4]	16.8 [0.0 - 188.8]	520.4 [389.6 - 670.4]	459.6 [318.0 - 689.0]	408.8 [287.6 - 641.0]	53.4 [19.0 - 237.2]	215.0 [39.4 - 423.2]	132.0 [15.2 - 380.4]
Mauritian	250	150	180	0.2 [0.0 - 102.6]	60.6 [0.0 - 225.4]	52.0 [0.0 - 275.6]	520.4 [389.6 - 670.4]	459.6 [318.0 - 689.0]	523.0 [353.2 - 841.0]	53.4 [19.0 - 237.2]	215.0 [39.4 - 423.2]	219.8 [20.0 - 524.0]
Mauritian	250	180	180	0.2 [0.0 - 102.6]	117.8 [0.6 - 318.0]	52.2 [0.0 - 275.6]	520.4 [389.6 - 670.4]	597.8 [395.6 - 878.6]	523.0 [353.2 - 841.0]	53.4 [19.0 - 237.2]	312.2 [76.0 - 571.0]	219.8 [20.0 - 524.0]
Chinese	200	60	60	4.0 [0.0 - 88.2]	1.2 [0.0 - 26.8]	0.2 [0.0 - 14.8]	482.6 [375.6 - 605.0]	160.0 [121.0 - 208.6]	154.4 [118.4 - 197.8]	76.4 [33.4 - 205.8]	33.4 [13.2 - 88.4]	23.0 [9.8 - 71.2]
Chinese	100	100	100	0.0 [0.0 - 0.8]	33.4 [0.2 - 130.4]	9.4 [0.0 - 107.2]	237.4 [185.6 - 289.4]	302.2 [216.2 - 434.8]	277.8 [206.4 - 407.2]	22.8 [13.8 - 38.6]	123.8 [33.4 - 254.0]	78.8 [20.2 - 226.0]
Chinese	200	100	100	4.0 [0.0 - 88.2]	34.4 [0.2 - 131.8]	9.4 [0.0 - 107.4]	482.6 [375.6 - 605.0]	302.6 [216.2 - 435.0]	277.8 [206.4 - 407.2]	76.4 [33.4 - 205.8]	124.0 [34.0 - 255.6]	78.8 [20.2 - 226.0]
Chinese	200	100	120	4.0 [0.0 - 88.2]	34.4 [0.2 - 131.8]	24.6 [0.0 - 175.6]	482.6 [375.6 - 605.0]	302.6 [216.2 - 435.0]	347.2 [263.2 - 558.6]	76.4 [33.4 - 205.8]	124.0 [34.0 - 255.6]	119.2 [26.2 - 324.4]
Chinese	200	100	150	4.0 [0.0 - 88.2]	34.4 [0.2 - 131.8]	63.2 [0.0 - 296.2]	482.6 [375.6 - 605.0]	302.6 [216.2 - 435.0]	466.6 [340.0 - 753.2]	76.4 [33.4 - 205.8]	124.0 [34.0 - 255.6]	211.2 [37.8 - 475.6]

Chinese	250	130	130	21.2 [0.0 - 158.6]	86.8 [2.8 - 223.4]	39.2 [0.0 - 188.8]	604.4 [470.0 - 758.6]	434.0 [300.6 - 628.6]	387.4 [280.0 - 597.4]	128.2 [48.0 - 306.2]	216.0 [64.4 - 394.4]	152.4 [28.8 - 368.4]
Chinese	150	150	150	0.2 [0.0 - 9.2]	123.4 [8.6 - 289.4]	67.2 [0.0 - 255.8]	356.8 [278.8 - 435.4]	527.2 [359.2 - 756.6]	464.4 [327.8 - 718.8]	41.4 [23.0 - 78.4]	284.0 [93.2 - 493.2]	214.2 [38.0 - 455.4]
Chinese	250	150	150	21.2 [0.0 - 158.6]	123.6 [8.8 - 290.2]	67.2 [0.0 - 255.8]	604.4 [470.0 - 758.6]	527.4 [359.4 - 758.6]	464.4 [328.0 - 719.0]	128.2 [48.0 - 306.2]	284.2 [93.4 - 493.4]	214.2 [38.0 - 455.4]
Chinese	250	150	180	21.2 [0.0 - 158.6]	123.6 [8.8 - 290.2]	119.4 [0.0 - 360.8]	604.4 [470.0 - 758.6]	527.4 [359.4 - 758.6]	593.6 [405.0 - 904.8]	128.2 [48.0 - 306.2]	284.2 [93.4 - 493.4]	305.4 [50.2 - 598.8]
Chinese	250	180	180	21.2 [0.0 - 158.6]	187.6 [21.0 - 396.4]	119.4 [0.0 - 360.8]	604.4 [470.0 - 758.6]	670.6 [454.4 - 958.2]	593.6 [405.0 - 904.8]	128.2 [48.0 - 306.2]	383.6 [145.6 - 639.0]	305.4 [50.4 - 598.8]

Table A2: Proportions of macaques with predicted plasmatic free trough concentration below the HF viruses EC50s, on day 1, day 7 and day 14 after treatment initiation. Five thousand individual profiles were simulated for each scenario.

Origin	**Dosing (mg/kg BID)**		**CCHFV, JUNV**			**LAV**			**EBOV**		
	D1	**D2-D14**	**D1**	**D7**	**D14**	**D1**	**D7**	**D14**	**D1**	**D7**	**D14**
Mauritian	250	150	67.7%	12.1%	36.2%	88.9%	26.6%	51.1%	99.4%	67.3%	82.1%
Mauritian	250	180	67.7%	6.0%	25.1%	88.9%	14.6%	39.2%	99.4%	42.4%	65.2%
Chinese	200	100	44.3%	12.0%	35.0%	80.7%	37.7%	60.8%	99.6%	89.7%	94.2%
Chinese	250	150	19.7%	2.6%	14.9%	51.5%	9.5%	28.3%	94.9%	40.3%	61.8%

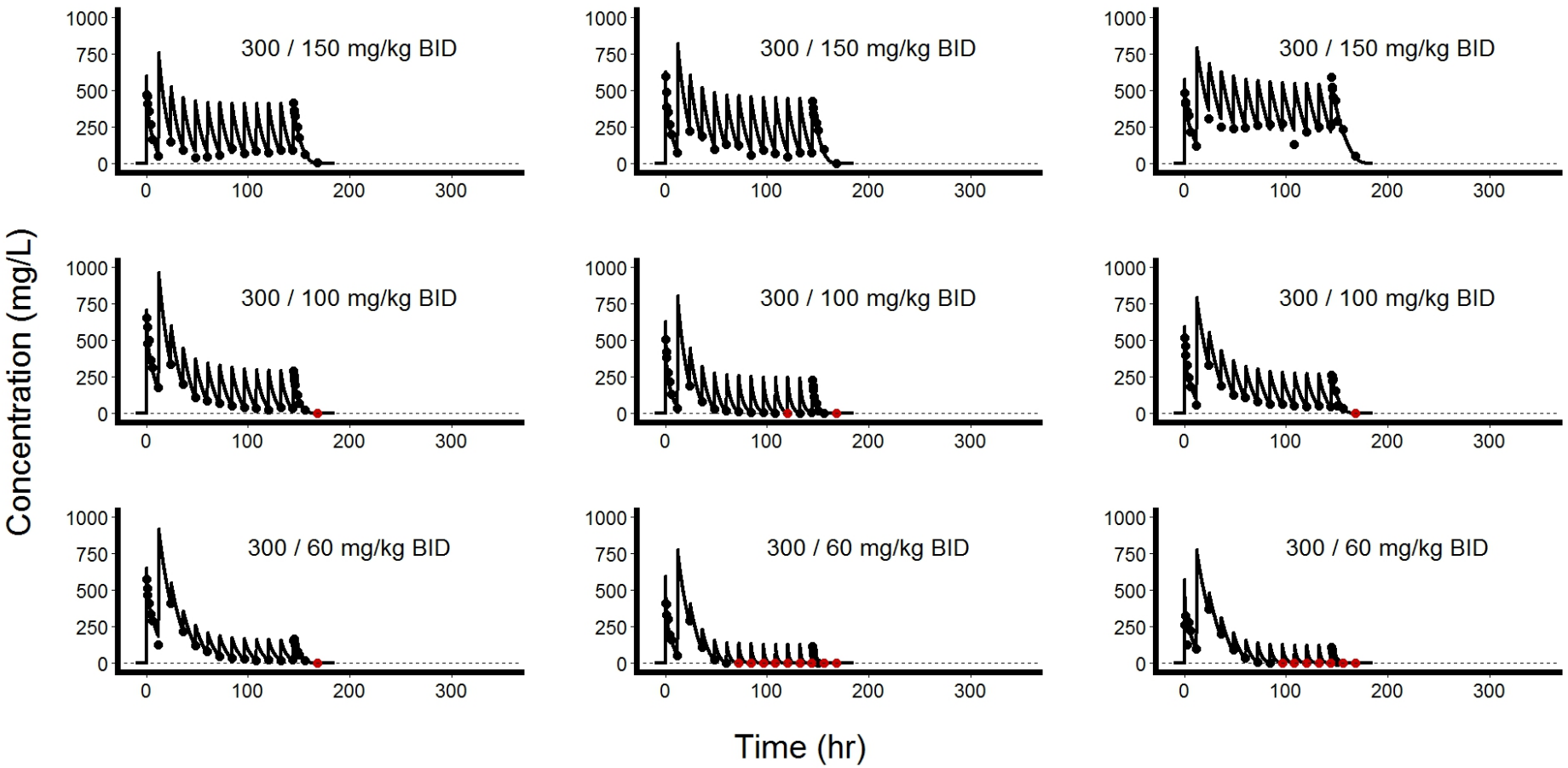
Concentration (mg/L)
300 / 150 mg/kg BID
300 / 100 mg/kg BID
300 / 60 mg/kg BID
1000
750
500
250
0
0
100
200
300
Time (hr)

Figure A5A

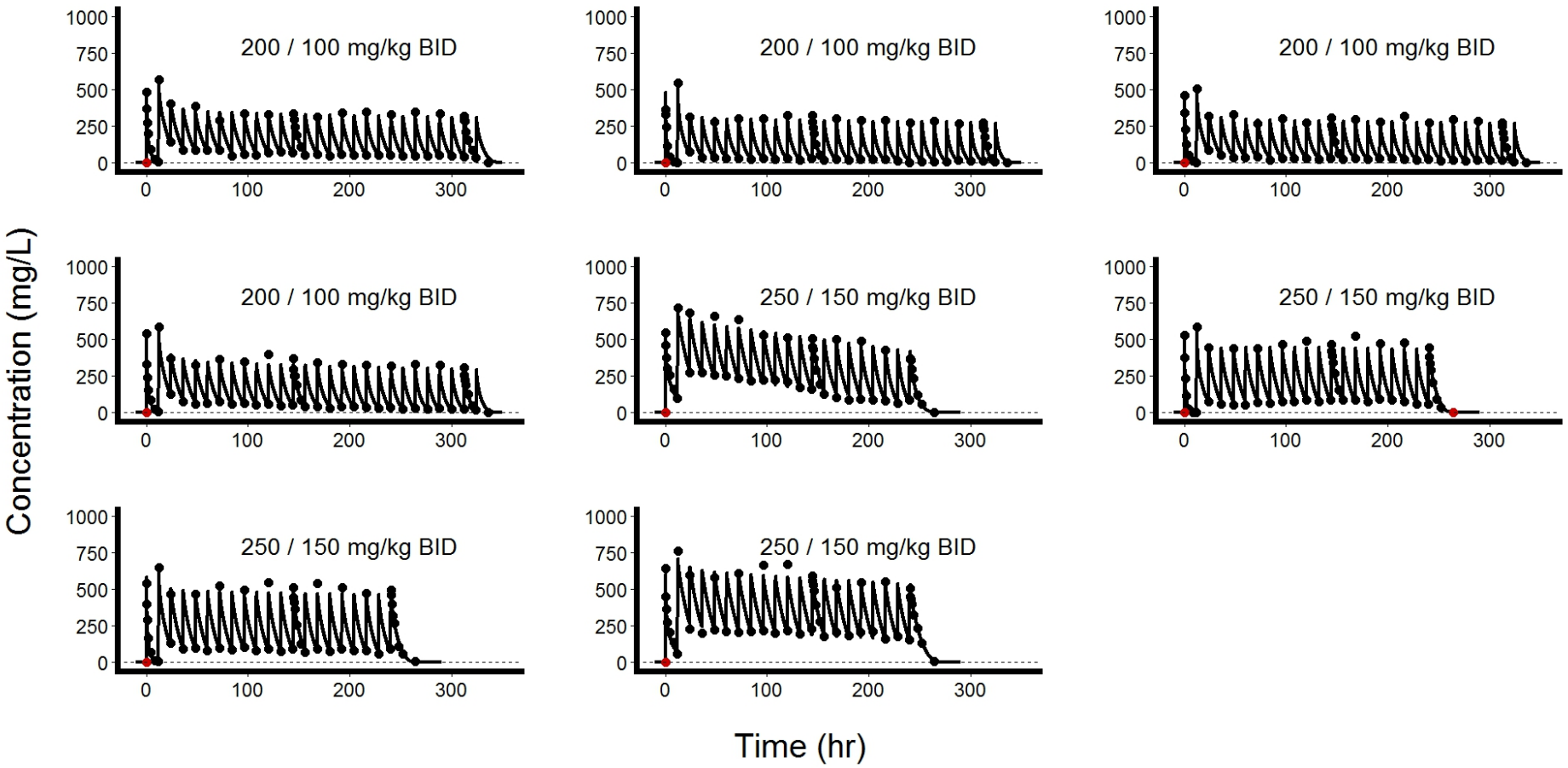
Concentration (mg/L)
Time (hr)
200 / 100 mg/kg BID
200 / 100 mg/kg BID
200 / 100 mg/kg BID
200 / 100 mg/kg BID
250 / 150 mg/kg BID
250 / 150 mg/kg BID
250 / 150 mg/kg BID
250 / 150 mg/kg BID
1000
750
500
250
0
0
100
200
300

Figure A5B

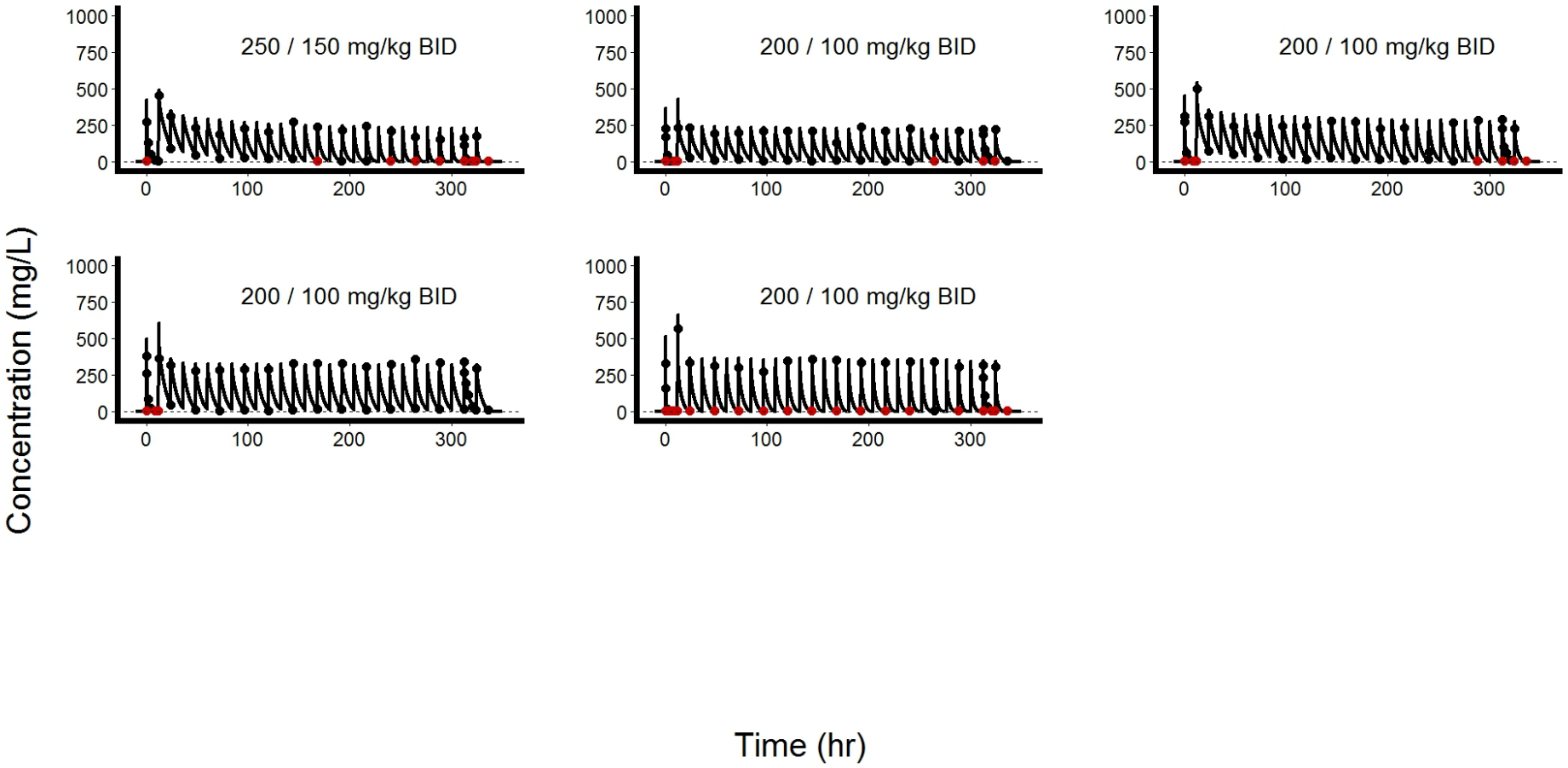
250 / 150 mg/kg BID
200 / 100 mg/kg BID
200 / 100 mg/kg BID
200 / 100 mg/kg BID
200 / 100 mg/kg BID
Concentration (mg/L)
Time (hr)
0
250
500
750
1000
0
100
200
300

Figure A5C

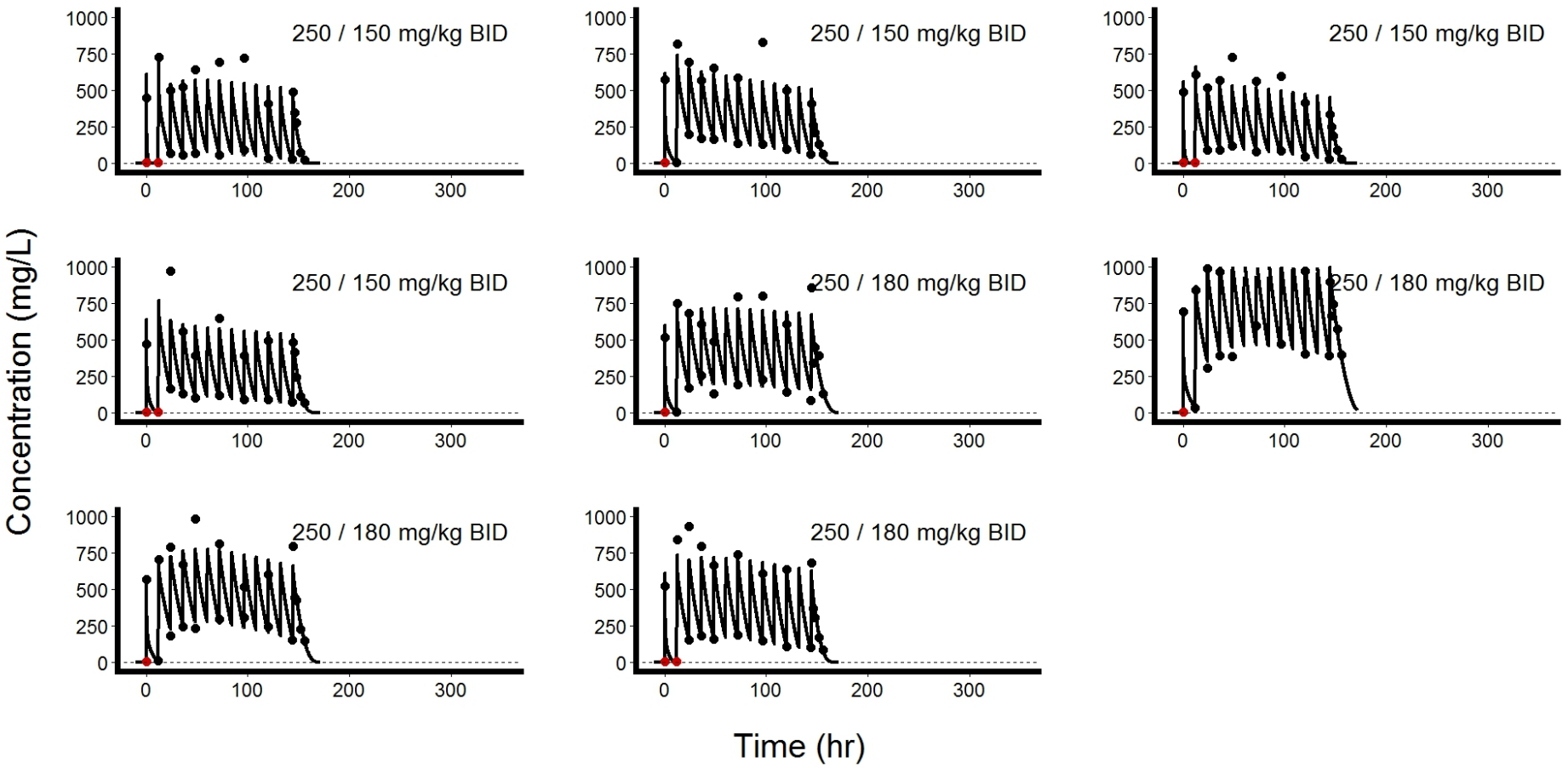

Figure A5D

Figure A5: Individual fits obtained with the enzyme inhibition pharmacokinetic model for study 1A (A), study 2A (B), study 1B (C) and study 2B (D). Loading dose on day 1 and maintenance dose are annotated for each cynomolgus macaque. Dots represent observations, solid line model predictions. Red dots stand for observation below the limit of quantitation.

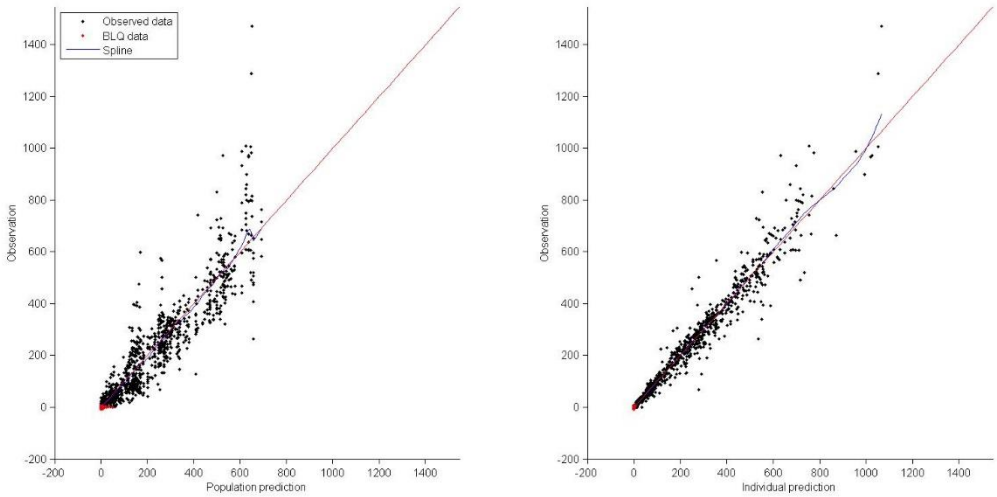

Figure A6: Observations vs population (left) and individual (right) predictions of final PK model. Red dots correspond to residuals of observations below the limit of quantitation.

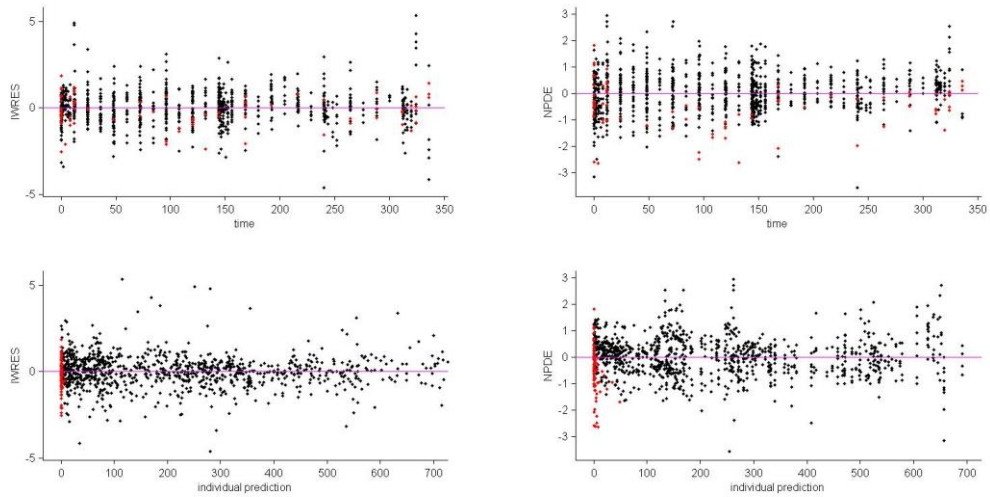

Figure A7: Individual weighted residuals (left) and npde (right) plotted vs time (top line) and vs individual predictions (bottom line) of final PK model. Red dots correspond to residuals of observations below the limit of quantitation.

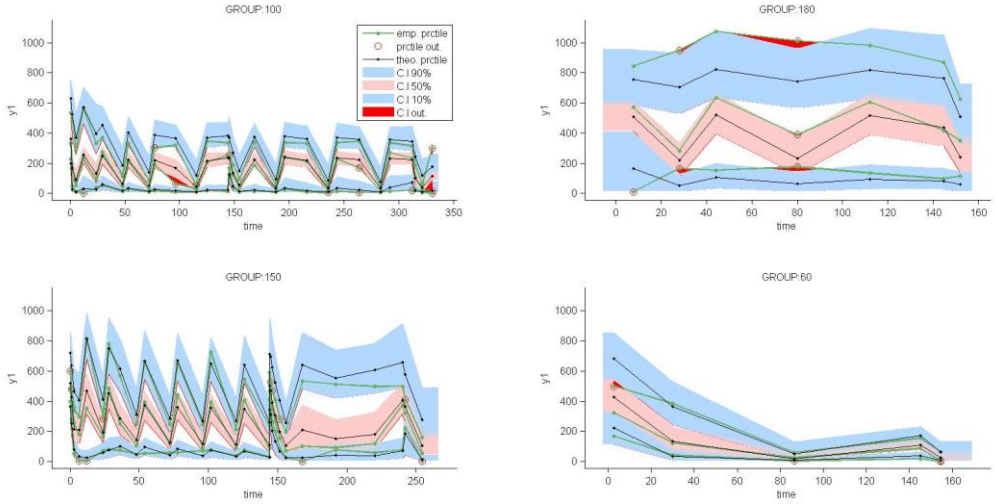

741

742 Figure A8: Visual predictive checks of the final PK model, stratified on maintenance doses.

743

744